Mathematical Biosciences and Engineering

http://www.aimspress.com/journal/MBE

MBE, 19(2): 1786–1824.
DOI: 10.3934/mbe.2022084
Received: 27 October 2021
Accepted: 14 December 2021
Published: 17 December 2021

Research article

Analysis of yellow fever prevention strategy from the perspective of mathematical model and cost-effectiveness analysis

Bevina D. Handari[1], Dipo Aldila [1,*], Bunga O. Dewi [1], Hanna Rosuliyana[1] and Sarbaz H. A. Khosnaw[2]

[1] Department of Mathematics, Universitas Indonesia, Kampus UI Depok, Depok 16424, Indonesia
[2] Department of Mathematics, University of Raparin, Ranya 46012, Kurdistan Region of Iraq

* **Correspondence:** Email: aldiladipo@sci.ui.ac.id.

Abstract: We developed a new mathematical model for yellow fever under three types of intervention strategies: vaccination, hospitalization, and fumigation. Additionally, the side effects of the yellow fever vaccine were also considered in our model. To analyze the best intervention strategies, we constructed our model as an optimal control model. The stability of the equilibrium points and basic reproduction number of the model are presented. Our model indicates that when yellow fever becomes endemic or disappears from the population, it depends on the value of the basic reproduction number, whether it larger or smaller than one. Using the Pontryagin maximum principle, we characterized our optimal control problem. From numerical experiments, we show that the optimal levels of each control must be justified, depending on the strategies chosen to optimally control the spread of yellow fever.

Keywords: yellow fever; vaccination; hospitalization; vector control; optimal control; cost-effectiveness

1. Introduction

Yellow fever is a hemorrhagic fever disease that is transmitted by the Aedes or Haemagogus aegypti infected mosquito, which contains the yellow fever virus. The virus that causes this disease belongs to the genus Flavivirus, a large group of RNA viruses. It is one of the most dangerous infectious diseases. The mortality rate of this disease ranges from 20 to 50%, but in severe cases, it can exceed 50%. There is no specific treatment for this disease, but it can be reduced through vaccination [1]. Although the vaccine for yellow fever is lifelong, a booster is needed to guarantee the efficacy of this vaccine to protect humans from infection.

Various interventions can be performed to suppress the spread of yellow fever. Based on [2], fumigation is the most recommended form of intervention to control mosquito populations. Even so,

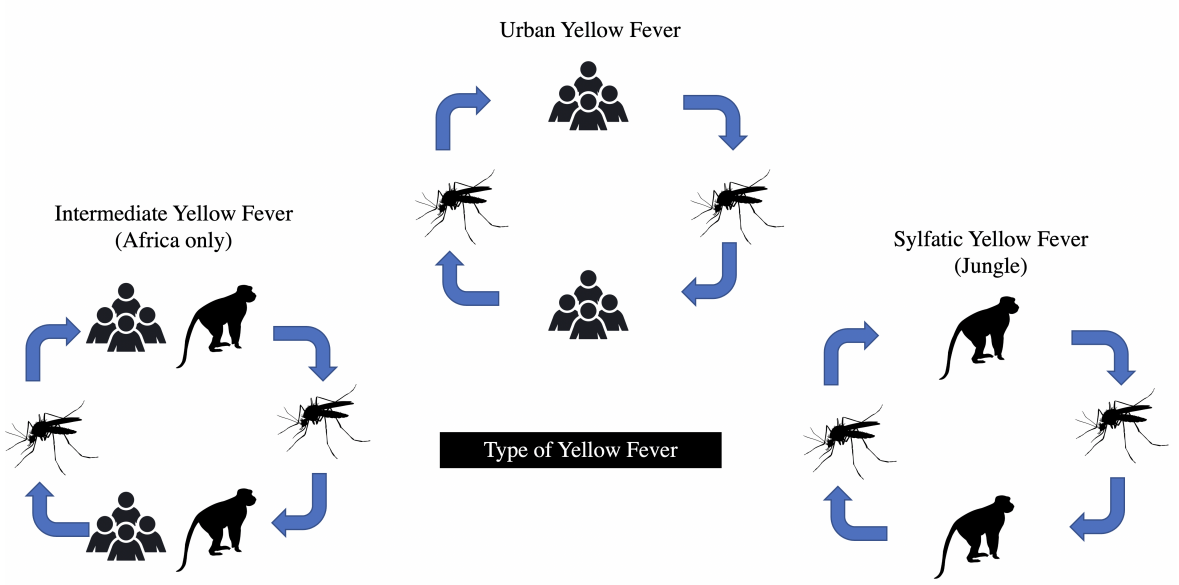

Figure 1. Type of yellow fever based on the transmission process.

this intervention needs to be carefully considered in its application in the field because it can trigger mosquito resistance to fumigation materials [3]. In addition to fumigation, vaccination is highly recommended, especially for tourists entering areas where yellow fever is endemic. Although it is claimed that yellow fever vaccination lasts forever, a vaccine booster must maintain the vaccine's ability to protect the individual from infection at maximum levels [4]. Although the yellow fever vaccine is claimed to reach the maximum protection at 4th week after the injection, the implementation of the yellow fever vaccine has some side effects for high-risk groups. These groups include infants aged 6–8 months, individuals more than 60 years old, pregnant, and breastfeeding women [3]. Despite the long history of safety, there are some cases of worsening effect of the use of yellow fever vaccine [1]. The author of [1] expresses more concern about yellow fever vaccine-associated neurotropic disease (YEL-AND) because it is fatal, despite the low number of reported cases.

Mathematical model have been used by many authors to model the dynamic of disease, whether it in human [5–9], animals [10], or plants [11, 12].Compared with other vector-borne diseases such as malaria or dengue, as far as we know, there are a few of mathematical models discussing yellow fever. The author of [13] introduced a yellow fever transmission model involving two types of hosts, namely, humans and primates. They found that their basic reproduction number consists of the addition of reproduction from human-mosquito interaction and primate (monkey)-mosquito interaction. Additionally, [14] introduced a yellow fever model that considers the vaccination of the human population and aquatic phase of the mosquito. Recently, [15] modified the model by [14] by adding a vertical transmission in the mosquito population to their model. Furthermore, they also involved treated bed nets, larvicides, and adulticides as alternative means of intervention. They showed that their model exhibits backward bifurcation phenomena that make the eradication program for yellow fever more difficult. A mathematical model was used to analyze the impact of vaccination for yellow fever in Angola, as analyzed by [16].

Based on the above description, we introduce a new mathematical model for yellow fever transmission, considering vaccination, fumigation, and treatment. We also include the possible side effects of

the yellow fever vaccine, which may lead to YEL-AND phenomena. Our model includes the aforementioned strategies as time-dependent variables. We aim to minimize the number of infected individuals keeping the cost of interaction as low as possible. Hence, the most cost-effective possible strategies are then analyzed using the cost-effectiveness method [17]. To our knowledge, this work is the first yellow fever model to consider the side effects of the yellow fever vaccine with a time-dependent intervention.

The remainder of this paper is organized as follows. In Section 2, we develop our model using time-dependent interventions. Treating the interventions as a constant parameter, we analyze our special case model regarding its equilibrium points and local stability criteria in Section 3. The characterization of the optimal control problem and its numerical experiments are presented in Section 4. The conclusions of our study are presented in Section 5.

2. The construction of the yellow fever optimal control model

In this study, we introduced a new mathematical model to describe the spread of yellow fever. Our model includes vaccination ($u_1(t)$), hospitalization ($u_2(t)$), and fumigation ($u_3(t)$) as time-dependent control variables. We aimed to understand the impact of the worsening effect of vaccination intervention on the dynamics of yellow fever and determine the best possible combination of cost-effective strategies in the yellow fever eradication policy effort.

First, we divide the total human population (denoted by $N(t)$) based on their health and vaccination status into eight compartments, namely, susceptible humans ($S(t)$), vaccinated humans ($V(t)$), unvaccinated exposed humans ($E_1(T)$), vaccinated exposed humans ($E_2(t)$), infected humans without vaccination worsening effect ($I(t)$), infected humans with worsening effect of vaccine ($T_1(t)$), infected humans who get worsening effect from the vaccine and were hospitalized ($T_2(t)$), and recovered humans ($R(t)$). Additionally, we divide the mosquito population into susceptible and infected mosquitoes, denoted by $U(t)$ and $W(t)$, respectively. Owing to the short life expectancy of mosquitoes, we exclude the recovered compartments of mosquitoes. This is because once the mosquitoes are infected by the yellow fever virus, they will stay infected forever. Hence, the total human and mosquito population at time t is expressed as follows:

$$\begin{aligned} N(t) &= S(t) + V(t) + E_1(t) + E_2(t) + I(t) + T_1(t) + T_2(t) + R(t), \\ M(t) &= U(t) + W(t). \end{aligned}$$

We use the transmission diagram in Figure 2 to construct our yellow fever model, and the description of the parameters is given in Table 1. For written simplification, we use $S, V, E_1, E_2, I, T_1, T_2, R, U$, and W instead of $S(t), V(t), E_1(t), E_2(t), I(t), T_1(t), T_2(t), R(t), U(t)$, and $W(t)$.

In our model, we assume that all recruitment rates enter the susceptible population through a constant rate Λ_h. Owing to a vaccination rate of u_1, the susceptible population will be transferred into compartment V. We assume that after a period of ω_h^{-1}, the effect of the vaccine disappears. Hence, the vaccinated individual was sent back to S. In our model, we assume that vaccination cannot provide perfect protection against yellow fever infection. Hence, there is an efficacy level of the vaccine, which is denoted by $1-\xi$. Thus, when a susceptible individual is infected with a success rate of β_h, vaccinated individuals will have a success probability of $\xi\beta_h$.

Susceptible individuals who are already infected will be classified into the exposed compartment E_1, which has no chance of experiencing any worsening vaccine effect. However, vaccinated individ-

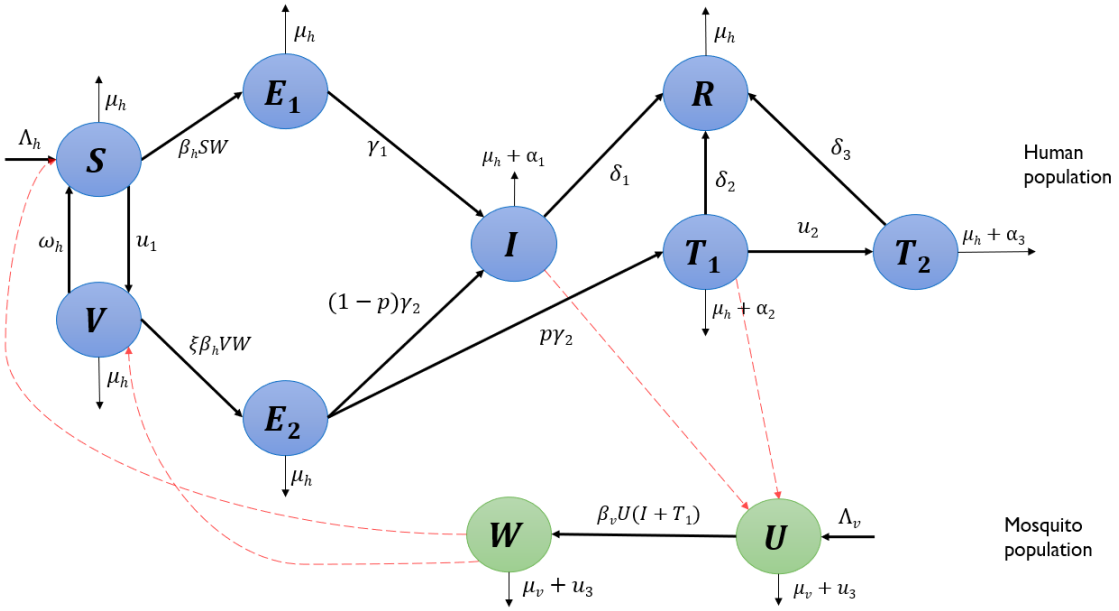

Figure 2. Transmission diagram of yellow fever for model in system (2.1).

uals who are already infected and experienced any worsening vaccine effect will be classified into the exposed compartment E_2. In our model, we assume that a yellow fever vaccine can have side effects on several types of individuals, including severely immunodeficient individuals, elderly individuals, pregnant women, newborns under six months of age, and individuals who already have thymic diseases, including thymoma and thymectomy [18]. These side effects can result in severe symptoms of infection. Because of this worsening effect, after the incubation period of γ_2^{-1}, an exposed individual E_2 will progress into infected stage I with a proportion of $1 - p$, where he/she has no worsening effect of the vaccine, and a proportion of p will progress to T_1 when he/she has the worsening effect of the vaccine. In contrast, the exposed individual E_1 progresses to I after the incubation period of γ_1^{-1}. Note that $\gamma_1^{-1} \leq \gamma_2^{-1}$.

Infected individuals in T_1 are assumed to have more severe symptoms than I individuals. Hence, individuals in T_1 must receive more intensive care in hospital. Therefore, we assume that there is a hospitalization rate of u_2 that will bring an individual in T_1 to a hospitalized individual in T_2. The infected individuals in I are assumed to recover from yellow fever after δ_1^{-1}, whereas T_1 and T_2 are assumed to recover after δ_1^{-1} and δ_2^{-1}, respectively. We assume that yellow fever may cause death in infected individuals I, T_1, and T_2 with a constant rate α_1, α_2, and α_3, respectively.

However, the mosquito population will increase because of a constant natural birth rate of Λ_v and decrease because of the natural death rate μ_v and fumigation u_3. All newborns in the mosquito population were assumed to be susceptible. Additionally, we assume that susceptible mosquitoes may get infected by biting infected individuals who do not go to the hospital, I and T_1, with a constant infection rate β_v.

Our aim is to understand how the spread of yellow fever may be reduced under three types of intervention: vaccination (u_1), hospitalization (u_2), and fumigation (u_3). In so many realities of disease eradication in the field, the limited costs of implementing interventions are always an unavoidable limitation. Therefore, instead of treating the above mentioned interventions as constant parameters, it

Table 1. Description of parameters in system (2.1).

Par	Description	Range	Ref.
Λ_h	Human recruitment rate	$\frac{10000}{65\times365}\frac{\text{human}}{\text{day}}$	Assumed
Λ_v	Mosquitoes recruitment rate	$\frac{20000}{30}\frac{\text{mosquitoes}}{\text{day}}$	Assumed
u_1	Vaccination rate	$[0,1]\frac{1}{\text{day}}$	[19–21]
u_2	Hospitalization rate	$[0,1]\frac{1}{\text{day}}$	Assumed
u_3	Fumigation rate	$[0,1]\frac{1}{\text{day}}$	[22,23]
ω_h	Waning rate of vaccine	$(0,1)\frac{1}{\text{day}}$	[19]
β_h	Mosquito-human infection rate	$[0.03,0.75]10^{-4}\frac{1}{\text{mosquito}\times\text{day}}$	[16,24]
$1-\xi$	Vaccine efficacy	[0.8-0.99]	[15,20,25]
β_v	Human-mosquito infection rate	$[0.15,1]10^{-5}\frac{1}{\text{human}\times\text{day}}$	[16,24]
μ_h	Natural death rate of human	$\frac{1}{65\times365}\frac{1}{\text{day}}$	[26]
μ_v	Natural death rate of mosquito	$\frac{1}{30}\frac{1}{\text{day}}$	[26]
γ_1	Progression rate of exposed humans who are not vaccinated	$0.331\frac{1}{\text{day}}$	[27]
γ_2	Progression rate of exposed human who are already vaccinated	$0.31\frac{1}{\text{day}}$	[27]
p	Proportion of exposed individuals who progressed into infectious but experienced side effects of the vaccine	[0,1]	Assumed
$\delta_1/\delta_2/\delta_3$	Recovery rate of $I/T_1/T_2$	$[0,0.143]\frac{1}{\text{day}}$	[27]
$\alpha_1/\alpha_2/\alpha_3$	Death rate because of yellow fever in $I/T_1/T_2$	$[0.2,0.5]10^{-3}\frac{1}{\text{day}}$	Assumed

would be better to make the intervention parameter both time-dependent and adaptive to the number of infected people and environmental conditions at time t. One approach is to find the optimal value of u_1 for each time t. This can be achieved by constructing a model to be discussed using an optimal control approach. Therefore, we discuss the time-dependent value of u_i, namely, $u_1(t), u_2(t)$, and $u_3(t)$.

Based on the above descriptions and formulations, the mathematical model of yellow fever under vaccination, hospitalization, and fumigation, as well as the worsening effect of vaccination, is given by the following system of ordinary differential equations:

$$\begin{aligned}
\frac{dS}{dt} &= \Lambda_h + \omega_h V - \beta_h S W - u_1(t)S - \mu_h S,\\
\frac{dV}{dt} &= u_1(t)S - \xi\beta_h V W - \mu_h V - \omega_h V,\\
\frac{dE_1}{dt} &= \beta_h S W - \gamma_1 E_1 - \mu_h E_1,\\
\frac{dE_2}{dt} &= \xi\beta_h V W - (1-p)\gamma_2 E_2 - p\gamma_2 E_2 - \mu_h E_2,\\
\frac{dI}{dt} &= \gamma_1 E_1 + (1-p)\gamma_2 E_2 - (\mu_h + \alpha_1)I - \delta_1 I,
\end{aligned} \tag{2.1}$$

$$\begin{aligned}
\frac{dT_1}{dt} &= p\gamma_2 E_2 - \delta_2 T_1 - u_2(t)T_1 - (\mu_h + \alpha_2)T_1,\\
\frac{dT_2}{dt} &= u_2(t)T_1 - \delta_3 T_2 - (\mu_h + \alpha_3)T_2,\\
\frac{dR}{dt} &= \delta_1 I + \delta_2 T_1 + \delta_3 T_2 - \mu_h R,\\
\frac{dU}{dt} &= \Lambda_v - \beta_v U(I + T_1) - (\mu_v + u_3(t))U,\\
\frac{dW}{dt} &= \beta_v U(I + T_1) - (\mu_v + u_3(t))W.
\end{aligned}$$

Note that the yellow fever model in system (2.1) is completed with non-negative initial conditions. Additionally, the parameters in system (2.1) are assumed to be non-negative.

This study aimed to minimize the number of infected individuals as much as possible while keeping the costs of vaccination, hospitalization, and fumigation as low as possible. Because we only want to minimize the number of infected individuals, we set the weight cost for S, V, R, and U, denoted by $\omega_1, \omega_2, \omega_8$, and ω_9, respectively, to zero. Hence, we describe our aim in the following cost function:

$$\mathcal{J}(u_i(t)) = \int_0^T \left(\omega_3 E_1 + \omega_4 E_2 + \omega_5 I + \omega_6 T_1 + \omega_7 T_2 + \omega_{10} W + \varphi_1 u_1^2 + \varphi_2 u_2^2 + \varphi_3 u_3^2\right) dt, \tag{2.2}$$

where φ_i for $i = 1, 2, 3$ denotes the weight cost for the control variables $u_1, u_2,$, and u_3, respectively. The interval $[0, T]$ represents the duration of the simulation time for the intervention that must be implemented. The total cost for interventions, such as vaccination, hospitalization, and fumigation, is presented as follows:

$$\int_0^T \left(\varphi_1 u_1^2 + \varphi_2 u_2^2 + \varphi_3 u_3^2\right) dt.$$

The quadratic cost function was chosen because of a convex function that ensures the existence of an optimal solution. On the other hand, the quadratic cost function is biologically interpreted as a nonlinear cost for intervention. For example, the cost of fumigation in a small area may only require a cost for buying the fumigation material and hiring an operator. However, when the area that needs to be fumigated becomes much wider, the cost includes not only the purchase of fumigation material and the hiring of operator, but also coordination costs, counseling before implementation, etc. Another quadratic cost function for another type of epidemiological optimal control model can be found in [28, 29]. On the other hand, all costs associated with the high number of infected humans and mosquitoes, which are not related to vaccination, hospitalization, or fumigation intervention were assumed to be proportional to the number of infected individuals, which is presented as follows:

$$\int_0^T \left(\omega_3 E_1 + \omega_4 E_2 + \omega_5 I + \omega_6 T_1 + \omega_7 T_2 + \omega_{10} W\right) dt.$$

Our model's aim is to minimize the number of infected individuals in human and mosquito populations while keeping the costs of vaccination, hospitalization, and fumigation as low as possible. Therefore, we seek to optimize the value of $\hat{u}_i$ for $i = 1, 2, 3$ such that

$$\mathcal{J}(\hat{u}_1, \hat{u}_2, \hat{u}_3) = \min_{u_1, u_2, u_3} \{\mathcal{J}(u_1, u_2, u_3) | u_i \in \mathcal{U}\}, \tag{2.3}$$

where

$$\mathcal{U} = \left\{(u_1, u_2, u_3)|u_i : [0, T] \to [u_i^{\min}, u_i^{\max}] \text{ is Lebesgue measurable}, i = 1, 2, 3, 4\right\}$$

is the admissible control set. Note that $u_i^{\min}$ and $u_i^{\max}$ for $i = 1, 2, 3$ represent the lower and upper bounds of each control variable, respectively.

3. Dynamical analysis of autonomous model

In this section, we analyze the autonomous version of system (2.1) regarding its existence and local stability criteria of equilibrium points, the form of the basic reproduction number, and bifurcation analysis. To accomplish this, let us assume that all control variables remain constant over time. Hence, using $u_1(t) = u_1, u_2(t) = u_2$, and $u_3(t) = u_3$, the autonomous version of system (2.1) is given by:

$$\begin{aligned}
\frac{dS}{dt} &= \Lambda_h + \omega_h V - \beta_h S W - u_1 S - \mu_h S,\\
\frac{dV}{dt} &= u_1 S - \xi\beta_h V W - \mu_h V - \omega_h V,\\
\frac{dE_1}{dt} &= \beta_h S W - \gamma_1 E_1 - \mu_h E_1,\\
\frac{dE_2}{dt} &= \xi\beta_h V W - (1-p)\gamma_2 E_2 - p\gamma_2 E_2 - \mu_h E_2,\\
\frac{dI}{dt} &= \gamma_1 E_1 + (1-p)\gamma_2 E_2 - (\mu_h + \alpha_1) I - \delta_1 I,\\
\frac{dT_1}{dt} &= p\gamma_2 E_2 - \delta_2 T_1 - u_2 T_1 - (\mu_h + \alpha_2) T_1,\\
\frac{dT_2}{dt} &= u_2 T_1 - \delta_3 T_2 - (\mu_h + \alpha_3) T_2,\\
\frac{dR}{dt} &= \delta_1 I + \delta_2 T_1 + \delta_3 T_2 - \mu_h R,\\
\frac{dU}{dt} &= \Lambda_v - \beta_v U(I + T_1) - (\mu_v + u_3) U,\\
\frac{dW}{dt} &= \beta_v U(I + T_1) - (\mu_v + u_3) W.
\end{aligned} \tag{3.1}$$

Hence, the dynamics of the total human population is given by

$$\frac{dN}{dt} = \Lambda_h - I\alpha_1 - T_1\alpha_2 - T_2\alpha_3 - \mu_h N,$$

and the dynamics of the total mosquito population is given by

$$\frac{dM}{dt} = \Lambda_v - (\mu_v + u_3) M.$$

3.1. Preliminary analysis

Before we begin analyzing the model in system (3.1) regarding the existence and stability of its equilibrium points, it is essential to ensure that the model in system (3.1) is well-defined biologically

and mathematically. That is, the solution in system (3.1) must always be non-negative for all $t > 0$. Properties related to these are written in the theorems below, where Theorem 1 deals with the positivity of the solution of each variable in system (3.1), and Theorem 2 discusses the upper bound of the total human and mosquito populations.

Theorem 1. *Given that the initial values of the system* (2.1) *are* $S(0)$, $V(0)$, $E_1(0)$, $E_2(0)$, $I(0)$, $T_1(0)$, $T_2(0)$, $R(0)$, $U(0)$, *and* $W(0) \geqslant 0$, *the solution of* $S(t)$, $V(t)$, $E_1(t)$, $E_2(t)$, $I(t)$, $T_1(t)$, $T_2(t)$, $R(t)$, $U(t)$, *and* $W(t)$ *will always be non-negative for all time* $t \geq 0$.

Proof. Please see Appendix A for the proof.

Theorem 2. *The total human* (N) *and mosquito* (M) *population in system (2.1) is eventually bounded as* $t \to \infty$.

Proof. The proof can be found in Appendix B.

Based on Theorems 1 and 2, we can conclude that each variable in system (3.1) is also bounded.

3.2. Yellow fever-free equilibrium point and the basic reproduction number

The purpose of this section is to determine the possible final state of the dynamics of system (3.1), which at times tends to infinity and is known as the equilibrium point. The equilibrium of system (3.1) is obtained by setting the right-hand side of system (3.1) to zero and solving this non-linear set of equations with respect to each variable on human and mosquito populations. The first equilibrium point of system (3.1) is the trivial point, known as the yellow fever-free equilibrium point ($\mathscr{E}_1$). This equilibrium point represents a situation in which all infected populations in humans and mosquitoes, as well as a recovered compartment in humans, do not exist. In this study, $\mathscr{E}_1$ is given as follows:

$$\begin{aligned} \mathscr{E}_1 &= (S^\dagger, V^\dagger, E_1^\dagger, E_2^\dagger, I^\dagger, T_1^\dagger, T_2^\dagger, R^\dagger, U^\dagger, W^\dagger), \\ &= \left(\frac{\Lambda_h(\mu_h + \omega_h)}{\mu_h(\mu_h + \omega_h + u_1)}, \frac{\Lambda_h u_1}{\mu_h(\mu_h + \omega_h + u_1)}, 0, 0, 0, 0, 0, 0, \frac{\Lambda_v}{\mu_v + u_3}, 0 \right). \end{aligned} \tag{3.2}$$

From the expressions of $S^\dagger$ and $V^\dagger$, $S^\dagger + V^\dagger = \frac{\Lambda_h}{\mu_h}$, which means that the existence of vaccination does not change the size of the total population at $\mathscr{E}_1$. Instead, it depends only on the number of newborns and the natural death rate. On the other hand, note that $\frac{S^\dagger}{V^\dagger} = \frac{\mu_h + \omega_h}{u_1}$. Our aim was to avoid the rapid spread of yellow fever by expecting many vaccinated individuals. In this study, this aim can be read as minimizing this ratio. To reduce the ratio of $S^\dagger$ to $V^\dagger$, we can either increase the number of vaccinated individuals (increasing the value of u_1) or improve vaccine quality by extending vaccine duration (reducing the value of ω_h). Additionally, note that the total number of mosquitoes at $\mathscr{E}_1$ is inversely proportional to the fumigation rate u_3. Hence, it is important to provide a large (but controlled) rate of fumigation to reduce the number of *aedes* mosquitoes. However, in many reports, uncontrolled fumigation may trigger a mosquito resistance to some fumigants [30].

Having the yellow fever-free equilibrium point in hand, as shown in Eq (3.2), we can calculate the basic reproduction number ($\mathscr{R}_0$) of system (3.1). In the context of our problem, the basic reproduction number presents an expected number of secondary yellow fever cases caused by one primary case during one infection period in a completely susceptible population. Several studies have demonstrated that basic reproduction numbers play an important role in determining the existence or extinction of

diseases in many epidemiological models [28,29,31]. These studies demonstrated that the disease will likely disappear if $\mathscr{R}_0 < 1$, and it must appear if $\mathscr{R}_0 > 1$. However, it is not always the case that $\mathscr{R}_0 < 1$ will always end in a situation where the disease disappears in the field. One of the causes is the occurrence of a backward bifurcation phenomenon in the model. When backward bifurcation occurs, $\mathscr{R}_0$ is no longer becomes a sufficient condition for the disappearance of a disease because the condition $\mathscr{R}_0 < 1$ causes a bistability phenomenon to occur. More examples of backward bifurcation phenomena arising from epidemiological models are available in [32].

Using the next-generation matrix approach [33], we have the basic reproduction number of the system (3.1) as follows:

$$\mathscr{R}_0 = \frac{\sqrt{\mu_h(\alpha_2 + \delta_2 + \mu_h + u_2)(\gamma_1 + \mu_h)M_1}}{\mu_h(\mu_h + \omega_h + u_1)(\gamma_2 + \mu_h)(\mu_v + u_3)(\gamma_1 + \mu_h)(\alpha_2 + \delta_2 + \mu_h + u_2)(\alpha_1 + \delta_1 + \mu_h)}, \tag{3.3}$$

with

$$\begin{aligned} M_1 =&(\gamma_1\mu_h^3 + ((\xi u_1 + \gamma_1)\gamma_2 + \gamma_1(\delta_2 + \omega_h + u_2 + \alpha_2))\mu_h^2 + (((\xi u_1 + \alpha_2 + \delta_2 + \omega_h + u_2)\gamma_1 + u_1(p\alpha_1 + p\delta_1 \\ &+ (\alpha_2 + \delta_2 + u_2)(1-p))\xi)\gamma_2 + \gamma_1\omega_h(\alpha_2 + \delta_2 + u_2))\mu_h + \gamma_1\gamma_2(u_1(p\alpha_1 + p\delta_1 + (\alpha_2 + \delta_2 + u_2)(1-p)) \\ &\xi + \omega_h(\alpha_2 + \delta_2 + u_2)))\Lambda_v\beta_v(\mu_h + \omega_h + u_1)(\gamma_2 + \mu_h)\beta_h(\alpha_1 + \delta_1 + \mu_h)\Lambda_h. \end{aligned}$$

The derivation of $\mathscr{R}_0$ is available in Appendix C. Using Theorem 2 in [34], the local stability criterion of $\mathscr{E}_1$ is given by the following theorem:

Theorem 3. *The yellow fev-free equilibrium point of system* (3.1) *is locally asymptotically stable if* $\mathscr{R}_0 < 1$*, and unstable if* $\mathscr{R}_0 > 1$.

Proof. Please see Appendix D for the proof.

3.3. The yellow fever endemic equilibrium

In this section, we analyze the existence of the non-trivial equilibrium point of system (3.1). The other equilibrium point of system (3.1) besides the yellow fever-free equilibrium point is the yellow fever endemic equilibrium point, which is given by the following expression:

$$\mathscr{E}_2 = (S^\ddagger, V^\ddagger, E_1^\ddagger, E_2^\ddagger, I^\ddagger, T_1^\ddagger, T_2^\ddagger, R^\ddagger, U^\ddagger, W^\ddagger),$$

where

$$
\begin{aligned}
S^{\ddagger} &= \frac{\Lambda_h\left(W^{\ddagger}\xi\beta_h+\mu_h+\omega_h\right)}{W^{\ddagger 2}\xi{\beta_h}^2+((\xi+1)\mu_h+\xi u_1+\omega_h)W^{\ddagger}\beta_h+\mu_h(\mu_h+\omega_h+u_1)},\\
V^{\ddagger} &= \frac{u_1\Lambda_h}{W^{\ddagger 2}\xi{\beta_h}^2+((\xi+1)\mu_h+\xi u_1+\omega_h)W^{\ddagger}\beta_h+\mu_h(\mu_h+\omega_h+u_1)},\\
E_1^{\ddagger} &= \frac{W^{\ddagger}\Lambda_h\beta_h\left(W^{\ddagger}\xi\beta_h+\mu_h+\omega_h\right)}{(\gamma_1+\mu_h)({\mu_h}^2+(W^{\ddagger}(\xi+1)\beta_h+\omega_h+u_1))\mu_h+W^{\ddagger}\beta_h(W^{\ddagger}\xi\beta_h+\xi u_1+\omega_h)},\\
E_2^{\ddagger} &= \frac{u_1\beta_h\Lambda_h\xi W^{\ddagger}}{(\gamma_2+\mu_h)\left(W^{\ddagger 2}\xi{\beta_h}^2+((\xi+1)\mu_h+\xi u_1+\omega_h)\right)W^{\ddagger}\beta_h+\mu_h(\mu_h+\omega_h+u_1)},\\
I^{\ddagger} &= \frac{\left(\gamma_1{\mu_h}^2+\left((u_1(1-p)\xi+\gamma_1)\gamma_2+\gamma_1\left(W^{\ddagger}\xi\beta_h+\omega_h\right)\right)\right)\mu_h+\gamma_1\left(W^{\ddagger}\xi\beta_h+u_1(1-p)\xi+\omega_h\right)\gamma_2)\beta_h W^{\ddagger}\Lambda_h}{(\gamma_1+\mu_h)(\alpha_1+\delta_1+\mu_h)(\gamma_2+\mu_h)({\mu_h}^2+(W^{\ddagger}(\xi+1)\beta_h+\omega_h+u_1))\mu_h+W^{\ddagger}\beta_h(W^{\ddagger}\xi\beta_h+\xi u_1+\omega_h)},\\
T_1^{\ddagger} &= \frac{p\gamma_2u_1\beta_h\Lambda_h\xi W^{\ddagger}}{({\mu_h}^2+(W^{\ddagger}(\xi+1)\beta_h+\omega_h+u_1)\mu_h+W^{\ddagger}\beta_h)((W^{\ddagger}\xi\beta_h+\xi u_1+\omega_h))(\alpha_2+\delta_2+\mu_h+u_2)(\gamma_2+\mu_h)},\\
T_2^{\ddagger} &= \frac{W^{\ddagger}p\xi\Lambda_h\beta_h\gamma_2u_1u_2}{(\alpha_3+\delta_3+\mu_h)({\mu_h}^2+(W^{\ddagger}(\xi+1)\beta_h+\omega_h+u_1))\mu_h+W^{\ddagger}\beta_h(W^{\ddagger}\xi\beta_h+\xi u_1+\omega_h)},\\
R^{\ddagger} &= \frac{\delta_1I^{\ddagger}+\delta_2T_1^{\ddagger}+\delta_3T_2^{\ddagger}}{\mu_h},\\
U^{\ddagger} &= \frac{\Lambda_v}{I^{\ddagger}\beta_v+T_1^{\ddagger}\beta_v+\mu_v+u_3},
\end{aligned}
\tag{3.4}
$$

where $W^{\ddagger}$ is taken from the positive roots of the following quadratic polynomial of W:

$$F(W) = a_2W^2 + a_1W + a_0 = 0, \tag{3.5}$$

with

$$
\begin{aligned}
a_2 =&\xi{\beta_h}^2(\mu_v+u_3)(\gamma_2+\mu_h)(\alpha_2+\delta_2+\mu_h+u_2)(\Lambda_h\beta_v\gamma_1+\alpha_1\gamma_1\mu_v+\alpha_1\gamma_1u_3+\alpha_1\mu_h\mu_v+\alpha_1\mu_hu_3+\delta_1\gamma_1\mu_v\\
&+\delta_1\gamma_1u_3+\delta_1\mu_h\mu_v+\delta_1\mu_hu_3+\gamma_1\mu_h\mu_v+\gamma_1\mu_hu_3+{\mu_h}^2\mu_v+{\mu_h}^2u_3),\\
a_1 =&\beta_h\beta_v\Lambda_h((((\mu_v+u_3){\mu_h}^2+(((\mu_v+u_3)u_1-\Lambda_v\beta_h)\xi+(\mu_v+u_3)(\alpha_2+\delta_2+\omega_h+u_2))\mu_h+((\mu_v+u_3)\\
&((1-p)(\alpha_2+\delta_2+u_2)+p(\alpha_1+\delta_1))u_1-\Lambda_v\beta_h(\alpha_2+\delta_2+u_2))\xi+\omega_h(\mu_v+u_3)(\alpha_2+\delta_2+u_2))\gamma_2+\mu_h\\
&(\alpha_2+\delta_2+\mu_h+u_2)((\mu_v+u_3)\mu_h-\xi\beta_h\Lambda_v+\omega_h(\mu_v+u_3)))\gamma_1+\mu_h(\mu_v+u_3)u_1\gamma_2\xi(\mu_h+(1-p)(\alpha_2\\
&+\delta_2+u_2)+p(\alpha_1+\delta_1))),\\
a_0 =&\mu_h(\mu_v+u_3)^2(\gamma_2+\mu_h)(\gamma_1+\mu_h)(\alpha_2+\delta_2+\mu_h+u_2)(u_1+\mu_h+\omega_h)(\alpha_1+\delta_1+\mu_h)(1-\mathscr{R}_0^2).
\end{aligned}
$$

Based on the expression of $F(W)$, we have the following theorem regarding the existence criteria of $\mathscr{E}_2$ in $\mathbb{R}^6_+$:

Theorem 4. *The yellow fever endemic equilibrium ($\mathscr{E}_2$) of system* (3.1) *always exists if $\mathscr{R}_0 > 1$, and no yellow fever endemic equilibrium otherwise.*

Proof. Please see Appendix E for the proof.

3.4. Forward bifurcation

In this section, we analyze the type of bifurcation of the yellow fever model in (3.1). In many classical models, forward bifurcation in epidemiological models indicates that $\mathscr{R}_0$ is a necessary condition to ensure disease extinction ([5,31,35–37]). However, in several epidemiological models [28,38–40], another type of bifurcation, namely, backward bifurcation, may appear. Under these circumstances, the condition of the basic reproduction number being less than unity is no longer became sufficient to guarantee the extinction of the disease. This is because when backward bifurcation phenomena arise, bistability phenomena may appear where stable endemic equilibrium exists together with the stable disease-free equilibrium.

To analyze the type of bifurcation of our model in (3.1), we use the result of Theorem 11 in [41], which is commonly known as the Castillo-Song bifurcation theorem. To apply this theorem, let us re-symbolize our variable from $S, V, E_1, E_2, I, T_1, T_2$, and R into x_i for $i = 1, 2 \ldots 10$, respectively. Hence, we now have the system (3.1) that reads as follows:

$$\begin{aligned}
g_1 &:= \Lambda_h - \beta_h x_1 x_{10} - \mu_h x_1 + \omega_h x_2 - u_1 x_1,\\
g_2 &:= u_1 x_1 - \xi \beta_h x_2 x_{10} - \mu_h x_2 - \omega_h x_2,\\
g_3 &:= \beta_h x_1 x_{10} - \gamma_1 x_3 - \mu_h x_3,\\
g_4 &:= \xi \beta_h x_2 x_{10} - (1-p)\gamma_2 x_4 - p\gamma_2 x_4 - \mu_h x_4,\\
g_5 &:= \gamma_1 x_3 + (1-p)\gamma_2 x_4 - (\mu_h + \alpha_1) x_5 - \delta_1 x_5,\\
g_6 &:= p\gamma_2 x_4 - \delta_2 x_6 - u_2 x_6 - (\mu_h + \alpha_2) x_6,\\
g_7 &:= u_2 x_6 - \delta_3 x_7 - (\mu_h + \alpha_3) x_7,\\
g_8 &:= \delta_1 x_5 + \delta_2 x_6 + \delta_3 x_7 - \mu_h x_8,\\
g_9 &:= \Lambda_v - \beta_v x_9 (x_5 + x_6) - (\mu_v + u_3) x_9,\\
g_{10} &:= \beta_v x_9 (x_5 + x_6) - (\mu_v + u_3) x_{10}.
\end{aligned} \tag{3.6}$$

Next, we choose β_h as the bifurcation parameter. Therefore, solving $\mathscr{R}_0^2 = 1$ with respect to β_h (an argument similar to the proof of Theorem 4), we obtain the following:

$$\beta_h^* = \frac{(\alpha_2 + \delta_2 + \mu_h + u_2)(\alpha_1 + \delta_1 + \mu_h)(\gamma_1 + \mu_h)(\mu_h + \omega_h + u_1)\mu_h(\gamma_2 + \mu_h)(\mu_v + u_3)^2}{Z_0 - \gamma_1(\mu_h + \omega_h)(\gamma_2 + \mu_h)(\alpha_2 + \delta_2 + \mu_h + u_2)\beta_v \Lambda_v \Lambda_h}, \tag{3.7}$$

where $Z_0 = u_1(\gamma_1 + \mu_h)(\mu_h + (\delta_1 - \delta_2 - u_2 + \alpha_1 - \alpha_2)p + \alpha_2 + \delta_2 + u_2)\gamma_2 \beta_v \Lambda_v \Lambda_h \xi$. Linearization of

system (3.6) at $\mathscr{E}_2$ with $\beta_h = \beta_h^*$ gives

$$\mathcal{J} = \begin{bmatrix} -\mu_h - u_1 & \omega_h & 0 & 0 & 0 & 0 & 0 & 0 & 0 & a_{110} \\ u_1 & -\mu_h - \omega_h & 0 & 0 & 0 & 0 & 0 & 0 & 0 & a_{210} \\ 0 & 0 & -\gamma_1 - \mu_h & 0 & 0 & 0 & 0 & 0 & 0 & a_{310} \\ 0 & 0 & 0 & -\gamma_2 - \mu_h & 0 & 0 & 0 & 0 & 0 & a_{410} \\ 0 & 0 & \gamma_1 & -(p-1)\gamma_2 & a_{55} & 0 & 0 & 0 & 0 & 0 \\ 0 & 0 & 0 & p\gamma_2 & 0 & a_{66} & 0 & 0 & 0 & 0 \\ 0 & 0 & 0 & 0 & 0 & u_2 & a_{77} & 0 & 0 & 0 \\ 0 & 0 & 0 & 0 & \delta_1 & \delta_2 & \delta_3 & -\mu_h & 0 & 0 \\ 0 & 0 & 0 & 0 & -\frac{\beta_v \Lambda_v}{\mu_v + u_3} & -\frac{\beta_v \Lambda_v}{\mu_v + u_3} & 0 & 0 & a_{99} & 0 \\ 0 & 0 & 0 & 0 & \frac{\beta_v \Lambda_v}{\mu_v + u_3} & \frac{\beta_v \Lambda_v}{\mu_v + u_3} & 0 & 0 & 0 & u_3 + \mu_v \end{bmatrix},$$

where

$$\begin{aligned}
a_{110} &= \frac{(\mu_h + \omega_h)(\alpha_2 + \delta_2 + \mu_h + u_2)(\alpha_1 + \delta_1 + \mu_h)(\gamma_1 + \mu_h)(\gamma_2 + \mu_h)(\mu_v + u_3)^2}{A\gamma_2 - \gamma_1\mu_h(\mu_h + \omega_h)(\alpha_2 + \delta_2 + \mu_h + u_2))\beta_v\Lambda_v}, \\
a_{210} &= \frac{\xi\,(\alpha_2 + \delta_2 + \mu_h + u_2)(\alpha_1 + \delta_1 + \mu_h)(\gamma_1 + \mu_h)(\gamma_2 + \mu_h)(\mu_v + u_3)^2 u_1}{A\gamma_2 - \gamma_1\mu_h(\mu_h + \omega_h)(\alpha_2 + \delta_2 + \mu_h + u_2))\beta_v\Lambda_v}, \\
a_{310} &= -\frac{(\mu_h + \omega_h)(\alpha_2 + \delta_2 + \mu_h + u_2)(\alpha_1 + \delta_1 + \mu_h)(\gamma_1 + \mu_h)(\gamma_2 + \mu_h)(\mu_v + u_3)^2}{A\gamma_2 - \gamma_1\mu_h(\mu_h + \omega_h)(\alpha_2 + \delta_2 + \mu_h + u_2))\beta_v\Lambda_v}, \\
a_{410} &= -\frac{\xi\,(\alpha_2 + \delta_2 + \mu_h + u_2)(\alpha_1 + \delta_1 + \mu_h)(\gamma_1 + \mu_h)(\gamma_2 + \mu_h)(\mu_v + u_3)^2 u_1}{A\gamma_2 - \gamma_1\mu_h(\mu_h + \omega_h)(\alpha_2 + \delta_2 + \mu_h + u_2))\beta_v\Lambda_v}, \\
a_{55} &= -\mu_h - \alpha_1 - \delta_1, \\
a_{66} &= -\delta_2 - u_2 - \mu_h - \alpha_2, \\
a_{77} &= -\delta_3 - \mu_h - \alpha_3, \\
a_{99} &= -u_3 - \mu_v,
\end{aligned}$$

and $A = ((-{\mu_h}^2 + (\xi u_1 - \alpha_2 - \delta_2 - \omega_h - u_2)\mu_h + ((\delta_2 + u_2 - \alpha_1 + \alpha_2 - \delta_1)p - \alpha_2 - \delta_2 - u_2)u_1\xi - \omega_h(\alpha_2 + \delta_2 + u_2))\gamma_1 + (-\mu_h + (\delta_2 + u_2 - \alpha_1 + \alpha_2 - \delta_1)p - \delta_2 - u_2 - \alpha_2)u_1\mu_h\xi)$. From the direct calculation, it can be shown that $\mathcal{J}$ has a simple zero eigenvalue, while the other nine eigenvalues are negative. Hence, we can use the center manifold theory to analyze the bifurcation of our yellow fever model.

Following the application of the Castillo-Song bifurcation theorem, we must calculate the right and left eigenvectors related to the zero eigenvalue. The right eigenvector of $\mathcal{J}$ at eigenvalue zero is given as follows:

$$\mathbf{w} = (w_1, w_2, w_3, w_4, w_5, w_6, w_7, w_8, w_9, w_{10})^T$$

where

$$w_1 = -\frac{(\delta_3 + \mu_h + \alpha_3)(\alpha_2 + \delta_2 + \mu_h + u_2)(\gamma_2 + \mu_h)\left(\xi\,\omega_h u_1 + {\mu_h}^2 + 2\,\omega_h\mu_h + {\omega_h}^2\right)}{\mu_h(\mu_h + \omega_h + u_1)u_1},$$

$$w_2 = -\frac{(\delta_3+\mu_h+\alpha_3)(\alpha_2+\delta_2+\mu_h+u_2)(\gamma_2+\mu_h)(\xi\mu_h+\xi u_1+\mu_h+\omega_h)}{(\mu_h+\omega_h+u_1)\mu_h},$$
$$w_3 = \frac{(\alpha_2+\delta_2+\mu_h+u_2)(\mu_h+\omega_h)(\gamma_2+\mu_h)(\delta_3+\mu_h+\alpha_3)}{u_1(\gamma_1+\mu_h)},$$
$$w_4 = (\delta_3+\mu_h+\alpha_3)(\alpha_2+\delta_2+\mu_h+u_2)\xi,$$
$$w_5 = \frac{(\alpha_2+\delta_2+\mu_h+u_2)(\delta_3+\mu_h+\alpha_3)\left(\gamma_1{\mu_h}^2+((\gamma_2+\omega_h)A_1)\right)}{(\gamma_1+\mu_h)(\alpha_1+\delta_1+\mu_h)u_1},$$
$$w_6 = (\delta_3+\mu_h+\alpha_3)\xi p\gamma_2,$$
$$w_7 = \xi u_2 p\gamma_2,$$
$$w_8 = \frac{(\alpha_2+\delta_2+\mu_h+u_2)\gamma_2(\delta_1(\delta_3+\mu_h+\alpha_3)(\alpha_2+\delta_2+\mu_h+u_2)+A_2)}{\mu_h(\alpha_1+\delta_1+\mu_h)},$$
$$w_9 = -\frac{\Lambda_v\beta_v\left({\mu_h}^2+(\xi u_1+\alpha_2+\delta_2+\omega_h+u_2)\mu_h+u_1A_3\right)}{u_1(\mu_v+u_3)^2(\gamma_1+\mu_h)(\alpha_1+\delta_1+\mu_h)},$$
$$w_{10} = \frac{\Lambda_v\beta_v\left({\mu_h}^2+(\xi u_1+\alpha_2+\delta_2+\omega_h+u_2)\mu_h+u_1A_3\right)}{u_1(\mu_v+u_3)^2(\gamma_1+\mu_h)(\alpha_1+\delta_1+\mu_h)},$$

with

$$\begin{aligned}
A_1 =&\gamma_1+\xi u_1\gamma_2(-p+1)\mu_h+\gamma_1(\xi(-p+1)u_1+\omega_h)\gamma_2,\\
A_2 =&p((\delta_3+\mu_h+\alpha_3)(\mu_h+\alpha_1)\delta_2+(-\alpha_3\alpha_2-\alpha_2\delta_3-\mu_h\alpha_2-\mu_h\alpha_3-\alpha_3u_2-\mu_h\delta_3-{\mu_h}^2-\mu_hu_2)\\
&\delta_1+u_2\delta_3(\mu_h+\alpha_1)),\\
A_3 =&((1-p)(u_2+\alpha_2+\delta_2)+p(\alpha_1+\delta_1))\xi+\omega_h(\alpha_2+\delta_2+u_2)\gamma_1+(((\delta_1-\delta_2-u_2+\alpha_1-\alpha_2)p\\
&+\mu_h+\alpha_2+\delta_2+u_2)\mu_hu_1\xi)\gamma_2+\gamma_1\mu_h(\mu_h+\omega_h)(\alpha_2+\delta_2+\mu_h+u_2)(\delta_3+\mu_h+\alpha_3).
\end{aligned}$$

However, the left eigenvector of $\mathcal{J}$ for eigenvalue zero is given as follows:

$$\mathbf{v} = (v_1, v_2, v_3, v_4, v_5, v_6, v_7, v_8, v_9, v_{10})$$

where

$$\begin{aligned}
v_1 =& v_2 = v_7 = v_8 = v_9 = 0,\\
v_3 =& \gamma_1,\\
v_4 =&\frac{(\gamma_1+\mu_h)(\mu_h+(1-p)(u_2+\alpha_2+\delta_2)+p(\alpha_1+\delta_1))\gamma_2}{(\gamma_2+\mu_h)(\alpha_2+\delta_2+\mu_h+u_2)},\\
v_5 =&\gamma_1+\mu_h,\\
v_6 =&\frac{\alpha_1\gamma_1+\alpha_1\mu_h+\delta_1\gamma_1+\delta_1\mu_h+\gamma_1\mu_h+{\mu_h}^2}{\alpha_2+\delta_2+\mu_h+u_2},\\
v_{10} =&\frac{(\gamma_1+\mu_h)(\alpha_1+\delta_1+\mu_h)(u_3+\mu_v)}{\Lambda_v\beta_v}.
\end{aligned}$$

Using the formula as follows:

$$\mathcal{A} = \sum_{k,i,j=1}^{n=10} v_k w_i w_j \frac{\partial^2 g_k}{\partial x_i \partial x_j}(0,0), \quad \mathcal{B} = \sum_{k,i,j=1}^{n=10} v_k w_i \frac{\partial^2 g_k}{\partial x_i \partial \beta^*}(0,0). \tag{3.8}$$

we have the following:

$$\mathcal{A} = -\frac{2\,(\alpha_3+\delta_3+\mu_h)^2(\gamma_1{\mu_h}^3+((\xi\,u_1+\gamma_1)\gamma_2+\gamma_1(\delta_2+\omega_h+u_2+\alpha_2))\mu_h{}^2+M_0)}{{u_1}^2(\mu_v+u_3)^2(\gamma_1+\mu_h)(\alpha_1+\delta_1+\mu_h)\mu_h(\mu_h+\omega_h+u_1)},$$

$$\mathcal{B} = \frac{\left(\xi\,\gamma_2 u_1\,(\gamma_1+\mu_h)\,(\delta_1-\delta_2-u_2+\alpha_1-\alpha_2)\,p+(\alpha_2+\delta_2+\mu_h+u_2)^2\,M_1\right)}{u_1(\mu_v+u_3)^2(\gamma_1+\mu_h)(\alpha_1+\delta_1+\mu_h)\mu_h(\mu_h+\omega_h+u_1)(\gamma_2+\mu_h)(\alpha_2+\delta_2+\mu_h+u_2)},$$

where $M_1 = \left(\xi\,\gamma_1\gamma_2u_1+\xi\,\gamma_2\mu_hu_1+\gamma_1\gamma_2\mu_h+\gamma_1\gamma_2\omega_h+\gamma_1{\mu_h}^2+\gamma_1\mu_h\omega_h\right)(\alpha_3+\delta_3+\mu_h)\,\Lambda_v\Lambda_h\beta_v$ while $M_0 > 0$ cannot be shown in this study because of its long expression. Because we always have $\mathcal{A} < 0$ and $\mathcal{B} > 0$, we have the following results.

Theorem 5. *The yellow fever model in system* (3.1) *always exhibits a forward bifurcation at* $\mathcal{R}_0 = 1$.

Based on Theorem 5, we understand that $\mathcal{E}_2$ is locally asymptotically stable when $\mathcal{R}_0 > 1$ but is close to one. Additionally, based on our proposed model, we can conclude that a basic reproduction number less than unity will always ensure the extinction of yellow fever from the population.

3.5. Sensitivity analysis, bifurcation and autonomous simulation

In this section, we perform some numerical experiments based on our previous results on Theorems 3, 4, and 5. First, we analyze the elasticity of each parameter in $\mathcal{R}_0$ to determine the most influential parameter for changing the size of $\mathcal{R}_0$. Based on this result, we continue our simulation by showing the level set of $\mathcal{R}_0$ with respect to each control variable to understand the sensitivity of each parameter. The forward bifurcation diagram shows the impact of $\mathcal{R}_0$ on the endemic size of the infected mosquito population. Finally, numerical experiments were conducted to demonstrate the dynamic behavior of the system (3.1) under certain scenarios.

To conduct the elasticity analysis of $\mathcal{R}_0$ with respect to any parameter ρ, we use the following equation [42]:

$$\epsilon^{\rho}_{\mathcal{R}_0} = \frac{\partial \mathcal{R}_0}{\partial \rho} \times \frac{\rho}{\mathcal{R}_0}. \tag{3.9}$$

To perform these experiments, we use the following parameter values:

$$\Lambda_h = \frac{10000}{65\times 365}, \Lambda_v = \frac{20000}{30}, \beta_h = 10^{-5}, \beta_v = 10^{-5}, \xi = 0.05, \omega_h = 0.1, \mu_h = \frac{1}{65\times 365}, \mu_v = \frac{1}{30},$$
$$\gamma_1 = 0.31, \gamma_2 = 0.31, p = 0.1, \delta_1 = 0.143, \delta_2 = 0.0715, \delta_3 = 0.10725,$$
$$\alpha_1 = 0.00035, \alpha_2 = 0.0004375, \alpha_3 = 0.0002625, u_1 = 0.01, u_2 = 0.01, u_3 = 0.01,$$

which gives $\mathcal{R}_0 = 1.504$. Using the Eq (3.9), the elasticity of $\mathcal{R}_0$ with respect to each parameter in the system (3.1) with the value of the above parameter is shown in Table 2. Note that because α_3 and δ_3 do not appear in the expression of $\mathcal{R}_0$, $\epsilon^{\alpha_3}_{\mathcal{R}_0}$ and $\epsilon^{\delta_3}_{\mathcal{R}_0}$ are both zero. The positive sign of $\epsilon^{\rho}_{\mathcal{R}_0}$ means that $\mathcal{R}_0$ increases when ρ increases. However, when $\epsilon^{\rho}_{\mathcal{R}_0}$ is negative, $\mathcal{R}_0$ decreases as ρ increases. Hence, all control variables can reduce the value of $\mathcal{R}_0$ whenever these control parameters increase. The value of $\epsilon^{\rho}_{\mathcal{R}_0}$ represents the percentage of increase or decrease of $\mathcal{R}_0$ for a 1% increase or decrease in ρ. For example, because $\epsilon^{u_3}_{\mathcal{R}_0} = -0.2308$, a 1% increase in u_3 will reduce $\mathcal{R}_0$ by 0.2308%. Additionally, note that $|\epsilon^{u_3}_{\mathcal{R}_0}| = \max\left\{|\epsilon^{u_1}_{\mathcal{R}_0}|, |\epsilon^{u_2}_{\mathcal{R}_0}|, |\epsilon^{u_3}_{\mathcal{R}_0}|\right\}$. Hence, we conclude that fumigation is more

essential in reducing $\mathscr{R}_0$ compared to vaccination and hospitalization. These results are in accordance with the recommendations of the WHO regarding fumigation as one of the most recommended efforts to overcome yellow fever [3].

Table 2. Elasticity of $\mathscr{R}_0$ with respect to each parameter in system (3.1).

$\epsilon_{\mathscr{R}_0}^{\Lambda_h}$	$\epsilon_{\mathscr{R}_0}^{\Lambda_v}$	$\epsilon_{\mathscr{R}_0}^{\beta_h}$	$\epsilon_{\mathscr{R}_0}^{\beta_v}$	$\epsilon_{\mathscr{R}_0}^{\gamma_1}$	$\epsilon_{\mathscr{R}_0}^{\gamma_2}$
0.5	0.5	0.5	0.5	6.7×10^{-5}	3.64×10^{-7}
$\epsilon_{\mathscr{R}_0}^{\alpha_1}$	$\epsilon_{\mathscr{R}_0}^{\alpha_2}$	$\epsilon_{\mathscr{R}_0}^{\delta_1}$	$\epsilon_{\mathscr{R}_0}^{\delta_2}$	$\epsilon_{\mathscr{R}_0}^{\omega_h}$	$\epsilon_{\mathscr{R}_0}^{\xi}$
-0.0012	-2.32×10^{-6}	-0.49	-0.00038	0.043	0.0027
$\epsilon_{\mathscr{R}_0}^{\mu_h}$	$\epsilon_{\mathscr{R}_0}^{\mu_v}$	$\epsilon_{\mathscr{R}_0}^{p}$	$\epsilon_{\mathscr{R}_0}^{u_1}$	$\epsilon_{\mathscr{R}_0}^{u_2}$	$\epsilon_{\mathscr{R}_0}^{u_3}$
-0.5002	-0.77	0.000186	-0.043	-0.000053	-0.2308

In addition to understanding the impact of all parameters in Eq (2.1) to $\mathscr{R}_0$, we must understand the impact of these parameters on the dynamics of all variables in Eq (2.1). Hence, we conducted a sensitivity analysis using three methods: non-normalization, half normalization, and full normalization using the SimBiology toolbox for MATLAB [43, 44].

Suppose that the yellow fever model in Eq (2.1) has 10 compartments, x_i in $i = 1, 2, ..., 10$ represents $S, V, E_1, E_2, I, T_1, T_2, R, U$, and W, respectively. Furthermore, let k_j for $j = 1, 2, ..., 20$ represent all the parameters in system (2.1). We assume that the model-balanced equations are expressed as a system of differential equations as follows:

$$\frac{dx_i}{dt} = f_i(x, k), \tag{3.10}$$

where $x \in \mathbb{R}^n$, $k \in \mathbb{R}^m$, and $f_i(x, k)$ is the right-hand side of the system (2.1). The non-normalization sensitivities are given as follows:

$$\mathcal{S}_{k_j}^{x_i} = \frac{\partial x_i}{\partial k_j}, \tag{3.11}$$

where $\mathcal{S}_{k_j}^{x_i}$ is the sensitivity coefficient of each x_i with respect to each parameter k_j. The half-normalization sensitivities are also given by the following equation:

$$\mathcal{S}_{k_j}^{x_i} = \Big(\frac{1}{x_i}\Big)\Big(\frac{\partial x_i}{\partial k_j}\Big). \tag{3.12}$$

Furthermore, the full-normalization sensitivities are defined as follows:

$$\mathcal{S}_{k_j}^{x_i} = \Big(\frac{k_j}{x_i}\Big)\Big(\frac{\partial x_i}{\partial k_j}\Big). \tag{3.13}$$

The results of the sensitivity analysis without normalization are shown in Figure 3. The results shown in Figure 3 show that the infection parameters β_h and β_v are very dominant in influencing changes in the populations of S and E_1 in humans, and the populations of U and W on mosquitoes. This agrees with the results of the analysis in Table 2 regarding the effect of β_h and β_v, which are also dominant on $\mathscr{R}_0$. Furthermore, it was also observed that the fumigation intervention (u_3) was more dominant in suppressing the number of infected mosquitoes, whereas vaccination (u_2) was dominant

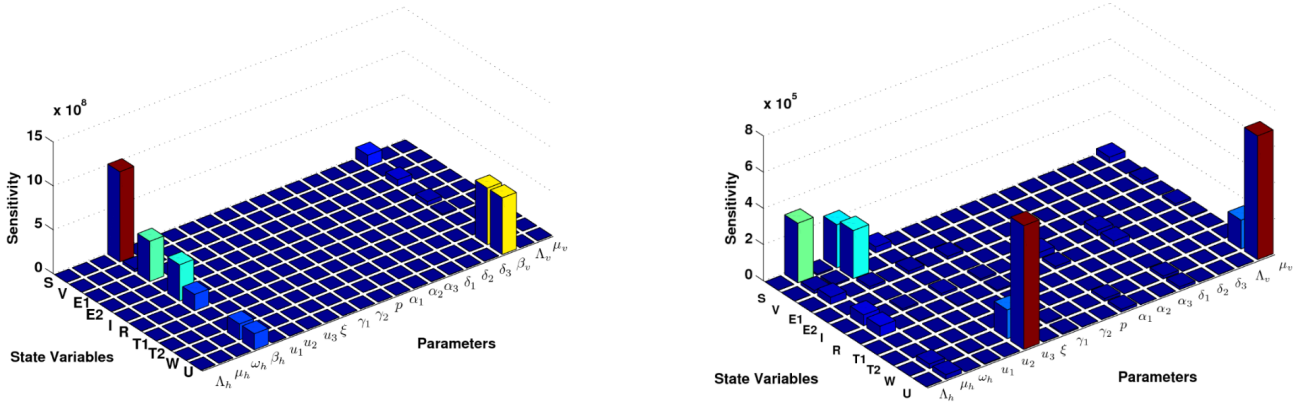

(a) **(b)**

Figure 3. Local sensitivity analysis with non–normalization technique of all variables with respect to (a) all parameters in computational simulations and (b) all parameters except β_h and β_v.

in determining the dynamics of healthy and vaccinated human populations. The simulation results in Figure 3 also confirm that hospitalization is the least effective among all control parameters.

We perform a half-normalization of our model in Figure 4. Note that β_h and β_v are still dominant in determining the dynamics of the (3.1) model compared to other parameters. Interestingly, fumigation is not only dominant in regulating population changes in mosquitoes but also in infected human populations. Clearly, the presence of fumigation has a significant impact on the population of E_1. This is consistent with the fact that the expected effect of fumigation is a reduction in the number of new infections in the human population. Figure 5 shows the sensitivity analysis using the full normalization approach. The results indicate the same result as using the non-and half-normalization approaches, where fumigation is more dominant compared to other control parameters.

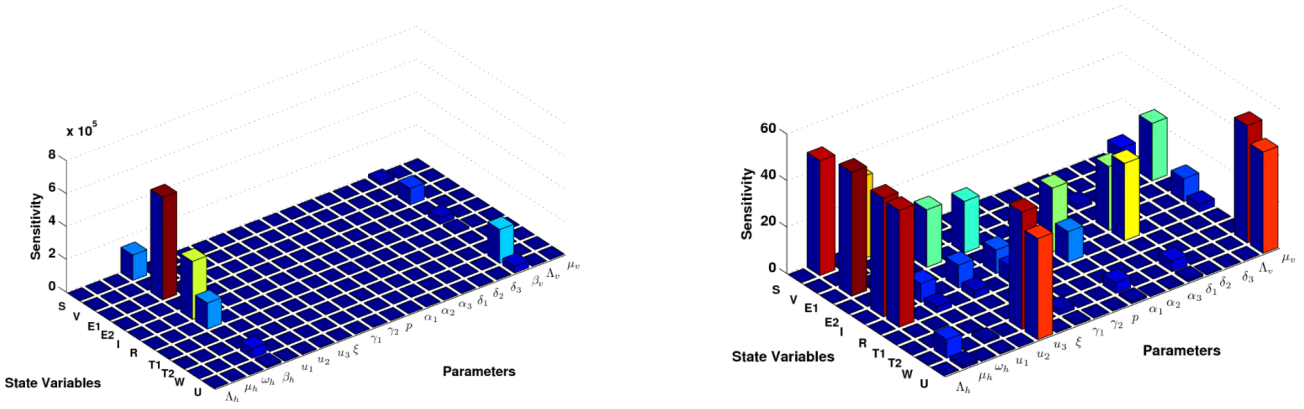

(a) **(b)**

Figure 4. Local sensitivity analysis with half–normalization technique of all variables with respect to (a) all parameters in computational simulations and (b) all parameters except β_h and β_v.

Next, we show the bifurcation diagram of system (3.1) using the same parameter values as in pre-

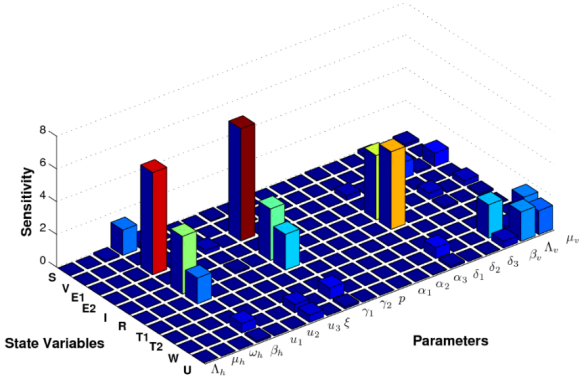

Figure 5. Local sensitivity analysis with full–normalization technique of all variables with respect to all parameters in computational simulations.

vious numerical experiments. We use our results in Theorem 5, which indicates that our proposed model in system (3.1) always exhibits a forward bifurcation at $\mathscr{R}_0 = 1$. The bifurcation diagram is shown in Figure 6. Note that the yellow fever-free equilibrium is always locally asymptotically stable when $\mathscr{R}_0 < 1$. At $\mathscr{R}_0 = 1$, the yellow fever-free equilibrium becomes unstable, while the yellow fever endemic equilibrium starts to arise and is locally asymptotically stable. Note that a larger value of $\mathscr{R}_0$ will increase the size of infected mosquitoes in an endemic equilibrium.

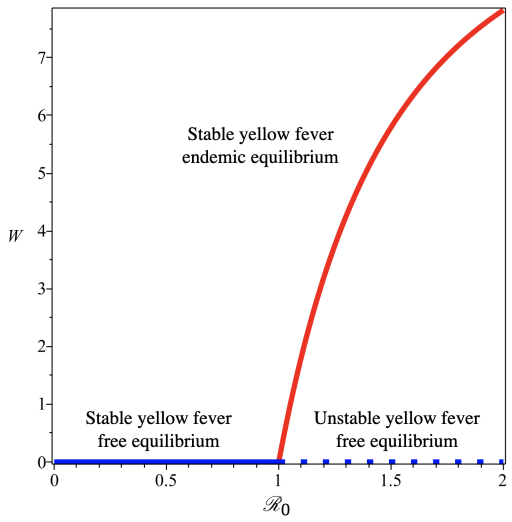

Figure 6. Bifurcation diagram of system (3.1) with respect to $\mathscr{R}_0$ and W.

To illustrate the dynamics of infected compartments with respect to the values of $\mathcal{R}_0$, we apply the Runge-Kutta method to solve system (3.1). In the first simulation we set the values of all parameter similar to the previous simulation, except $u_1 = 0.03, u_2 = 0.01, u_3 = 0.03$. This setting gives us $\mathcal{R}_0 < 1$. In Figure 7, we can see that all trajectories tend to the yellow fever free equilibrium point asymptotically, which in this case is given by

$$(S, V, E_1, E_2, I, T_1, T_2, R, U, W) = (7694, 2306, 0, 0, 0, 0, 0, 0, 10527, 0).$$

To simulate $\mathcal{R}_0 > 1$, we choose the same parameter value as before, except $\beta_h = 2 \times 10^{-5}, \beta_v = 2 \times 10^{-5}, u_1 = 0, u_2 = 0, u_3 = 0$. In Figure 8, we can see that all solutions tend to the endemic

equilibrium point, which is given by

$$(S, V, E_1, E_2, I, T_1, T_2, R, U, W) = (599, 0, 1.3, 0, 3, 0, 0, 9375, 19967, 33).$$

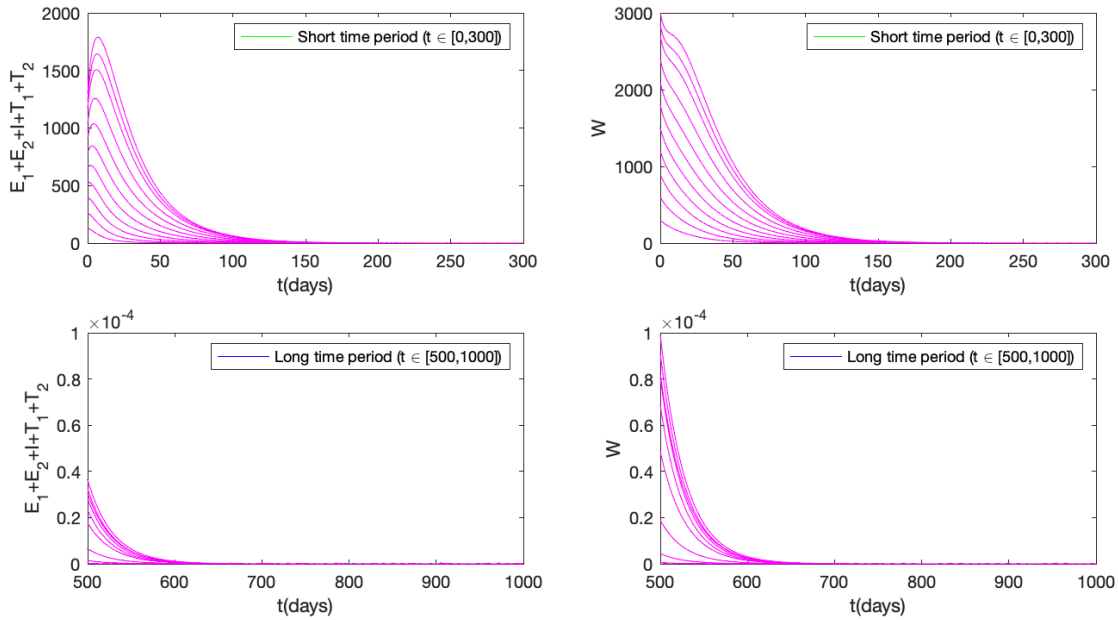

Figure 7. Dynamics of total infected human (left) and mosquito (right) for short (top) and long (bottom) time period which tend to the yellow fever free equilibrium for various initial conditions.

4. Characterization and simulation of the optimal control problem

4.1. Characterization of the optimal control problem

Optimal control has been used in several epidemiological models to analyze how the best form of intervention should be chosen to reduce the rate of spread of the disease, where the intervention is treated as a time-dependent variable [45–48]. In these studies, the optimal condition for the control variables concludes that the optimal dynamics of the controls depend on the population involved in the model. These various studies concluded that time-dependent interventions provide more optimal results in suppressing the spread of disease but at a more optimal cost.

Before we characterize our optimal control problem, we recall all the control variables introduced in Section 2 as follows:

- $u_1(t)$: Vaccination rate
- $u_2(t)$: Hospitalization rate
- $u_3(t)$: Fumigation rate.

The objective function is expressed using Eq (2.2). Our aim is to minimize the number of infected

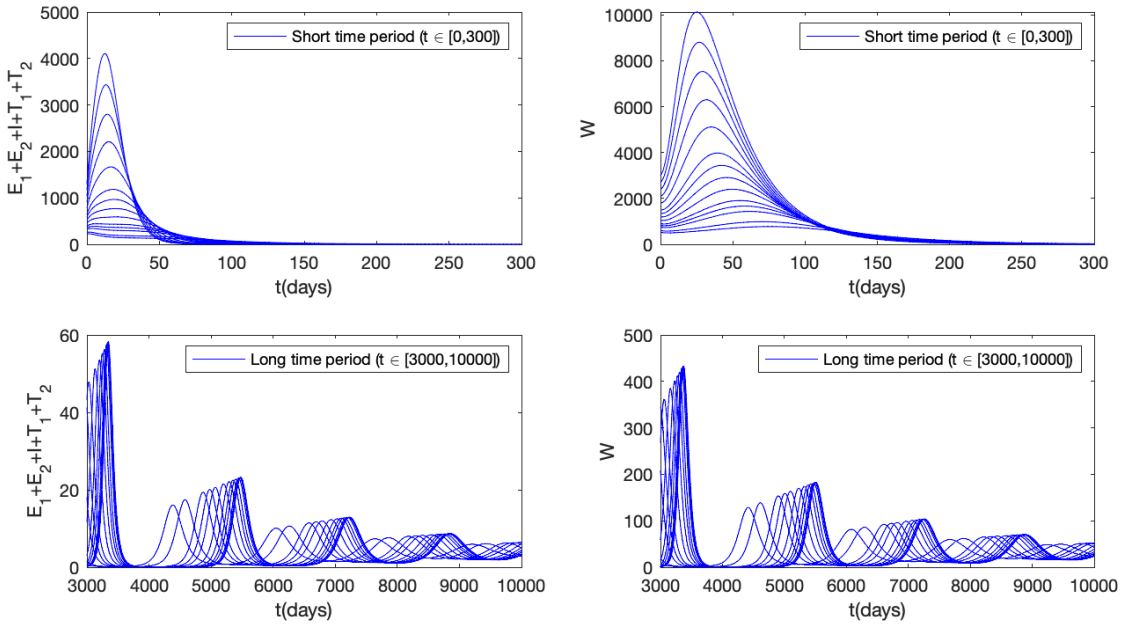

Figure 8. Dynamics of total infected human (left) and mosquito (right) for short (top) and long (bottom) time period which tend to the yellow fever endemic equilibrium for various initial conditions.

individuals with optimal interventions, which are read as follows:

$$\mathcal{J}(\hat{u}_1, \hat{u}_2, \hat{u}_3) = \min_{u_1,u_2,u_3} \{\mathcal{J}(u_1, u_2, u_3) | u_i \in \mathcal{U}\}, \tag{4.1}$$

where $\mathcal{U}$ is the admissible control set.

We use the Pontryagin maximum principle (PMP) [49] to determine the necessary condition for the existence of a triplet of our optimal controls. We define the Hamiltonian of the problem as follows:

$$\begin{aligned}\mathcal{H} =&\omega_3 E_1 + \omega_4 E_2 + \omega_5 I + \omega_6 T_1 + \omega_7 T_2 + \omega_{10} W + \varphi_1 u_1^2 + \varphi_2 u_2^2 + \varphi_3 u_3^2 + \lambda_1(\Lambda_h + \omega_h V - \beta_h S W \\ &- u_1 S - \mu_h S) + \lambda_2(u_1 S - \xi\beta_h V W - \omega_h V) + \lambda_3(\beta_h S W - \gamma_1 E_1 - \mu_h E_1) + \lambda_4(\xi\beta_h V W - \xi V \\ &- \mu_h V) + \lambda_5(\gamma_1 E_1 + (1-p)\gamma_2 E_2 - \delta_1 I - (\mu_h + \alpha_1) I) + \lambda_6(p\gamma_2 E_2 - \delta_2 T_1 - u_2 T_1 - (\mu_h + \alpha_2) T_1) \\ &+ \lambda_7(u_2 T_1 - \delta_3 T_2 - (\mu_h + \alpha_3) T_2) + \lambda_8(\delta_1 I + \delta_2 T_1 + \delta_3 T_2 - \mu_h R) + \lambda_9(\Lambda_v - \beta_v U(I + T_1) - \\ &(\mu_v + u_3) U) + \lambda_{10}(\beta_v U(I + T_1) - (\mu_v + u_3) W),\end{aligned} \tag{4.2}$$

where λ_i for $i = 1, 2, \ldots 10$ are the adjoint variables for the state variables $S, V, E_1, E_2, I, T_1, T_2, R, U$, and W, respectively. Hence, the necessary condition of our optimal control problem is given by the following theorem:

Theorem 6. *For the optimal control variables* $\hat{u}_1, \hat{u}_2,$ *and* $\hat{u}_3$, *and the optimal solutions* $\hat{S}, \hat{V}, \hat{E}_1, \hat{E}_2, \hat{I}, \hat{T}_1, \hat{T}_2, \hat{R}, \hat{U}$, *and* $\hat{W}$ *of system* (2.1), *the adjoint variables* λ_i *for* $i = 1, 2, \ldots 10$ *that*

satisfy the following:

$$\begin{aligned}
\dot{\lambda}_1 &= -\frac{\partial \mathcal{H}}{\partial S(t)} = \lambda_1(\beta_h W + u_1 + \mu_h) - \lambda_2 u_1 - \lambda_3 \beta_h I_v,\\
\dot{\lambda}_2 &= -\frac{\partial \mathcal{H}}{\partial V(t)} = -\lambda_1 \omega_h + \lambda_2(\xi\beta_h W + \omega_h + \mu_h) - \lambda_4 \xi \beta_h W,\\
\dot{\lambda}_3 &= -\frac{\partial \mathcal{H}}{\partial E_1(t)} = -\omega_3 + \lambda_3(\gamma_1 + \mu_h) - \lambda_5 \gamma_1,\\
\dot{\lambda}_4 &= -\frac{\partial \mathcal{H}}{\partial E_2(t)} = -\omega_4 + \lambda_4(\gamma_2 + \mu_h) - \lambda_5(1-p)\gamma_2 - \lambda_6 p\gamma_2,\\
\dot{\lambda}_5 &= -\frac{\partial \mathcal{H}}{\partial I(t)} = -\omega_5 + \lambda_5(\delta_1 + \mu_h + \alpha_1) - \lambda_8\delta_1 + \lambda_9\beta_v U - \lambda_{10}\beta_v U,\\
\dot{\lambda}_6 &= -\frac{\partial \mathcal{H}}{\partial T_1(t)} = -\omega_6 + \lambda_6(\delta_2 + u_2 + \mu_h + \alpha_2) - \lambda_7 u_2 - \lambda_8\delta_2 + \lambda_9\beta_v U - \lambda_{10}\beta_v U,\\
\dot{\lambda}_7 &= -\frac{\partial \mathcal{H}}{\partial T_2(t)} = -\omega_7 + \lambda_7(\delta_3 + \mu_h + \alpha_3) - \lambda_8\delta_3,\\
\dot{\lambda}_8 &= -\frac{\partial \mathcal{H}}{\partial R(t)} = \lambda_8\mu_h,\\
\dot{\lambda}_9 &= -\frac{\partial \mathcal{H}}{\partial U(t)} = \lambda_9(\beta_v I + \beta_v T_1 + \mu_v + u_3) - \lambda_{10}(\beta_v I + \beta_v T_1),\\
\dot{\lambda}_{10} &= -\frac{\partial \mathcal{H}}{\partial W(t)} = -\lambda_{10} + \lambda_1\beta_h S + \lambda_2\xi\beta_h V - \lambda_3\beta_h S - \lambda_4\xi\beta_h V + \lambda_{10}(\mu_v + u_3),
\end{aligned} \tag{4.3}$$

with transversality conditions $\lambda_i(T) = 0$ *for* $i = 1, 2, \ldots 10$. *Additionally, the controls* $\hat{u}_i$ *for* $i = 1, 2, 3$ *are given by the following:*

$$\begin{aligned}
\hat{u}_1(t) &= \begin{cases} 0 & ; \frac{S(\lambda_1-\lambda_2)}{2\varphi_1} \le 0,\\ 1 & ; \frac{S(\lambda_1-\lambda_2)}{2\varphi_1} \ge 1,\\ \frac{S(\lambda_1-\lambda_2)}{2\varphi_1} & ; \textit{others}. \end{cases}\\
\hat{u}_2(t) &= \begin{cases} 0 & ; \frac{T_1(\lambda_6-\lambda_7)}{2\varphi_2} \le 0,\\ 1 & ; \frac{T_1(\lambda_6-\lambda_7)}{2\varphi_2} \ge 1,\\ \frac{T_1(\lambda_6-\lambda_7)}{2\varphi_2} & ; \textit{others}. \end{cases}\\
\hat{u}_3(t) &= \begin{cases} 0 & ; \frac{U(\lambda_9+\lambda_{10})}{2\varphi_3} \le 0,\\ 1 & ; \frac{U(\lambda_9+\lambda_{10})}{2\varphi_3} \ge 1,\\ \frac{U(\lambda_9+\lambda_{10})}{2\varphi_3} & ; \textit{others}. \end{cases}
\end{aligned} \tag{4.4}$$

Proof. The adjoint system in Eq (4.3) is taken from the following formula

$$\begin{aligned}
&\dot{\lambda}_1 = -\frac{\partial \mathcal{H}}{\partial S}, \quad \dot{\lambda}_2 = -\frac{\partial \mathcal{H}}{\partial V}, \quad \dot{\lambda}_3 = -\frac{\partial \mathcal{H}}{\partial E_1}, \quad \dot{\lambda}_4 = -\frac{\partial \mathcal{H}}{\partial E_2}, \quad \dot{\lambda}_5 = -\frac{\partial \mathcal{H}}{\partial I},\\
&\dot{\lambda}_6 = -\frac{\partial \mathcal{H}}{\partial T_1}, \quad \dot{\lambda}_7 = -\frac{\partial \mathcal{H}}{\partial T_2}, \quad \dot{\lambda}_8 = -\frac{\partial \mathcal{H}}{\partial R}, \quad \dot{\lambda}_9 = -\frac{\partial \mathcal{H}}{\partial U}, \quad \dot{\lambda}_{10} = -\frac{\partial \mathcal{H}}{\partial W},
\end{aligned} \tag{4.5}$$

with the transversality condition $\lambda_i(T) = 0$ for $i = 1, 2 \dots 10$. To obtain the control characterization, we first take the derivative of $\mathcal{H}$ with respect to each control variable. Hence, we obtain the following:

$$\begin{aligned}\frac{\partial \mathcal{H}}{\partial u_1(t)} =& 2\varphi_1 u_1 - \lambda_1 S + \lambda_2 S,\\ \frac{\partial \mathcal{H}}{\partial u_2(t)} =& 2\varphi_2 u_2 - \lambda_6 T_1 + \lambda_7 T1,\\ \frac{\partial \mathcal{H}}{\partial u_3(t)} =& 2\varphi_2 u_3 - \lambda_9 U - \lambda_{10} I.\end{aligned}$$

Solve $\frac{\partial \mathcal{H}}{\partial u_i} = 0$ for each control variables, we have the following:

$$\begin{aligned}u_1^*(t) =& \frac{S(t)(\lambda_1 - \lambda_2)}{2\varphi_1},\\ u_2^*(t) =& \frac{T_1(t)(\lambda_6 - \lambda_7)}{2\varphi_2},\\ u_3^*(t) =& \frac{\lambda_9 U(t) + \lambda_{10} U(t)}{2\varphi_3}.\end{aligned}$$

Hence, based on the standard argument that $\hat{u}_i$ should be bounded between $u_i^{\min}$ and $u_i^{\max}$ (in this study, we choose $u_i^{\min} = 0, u_i^{\max} = 1$ for each control variable), we have Eq (4.4).

4.2. Numerical experiments

In this section, we perform numerical simulations for the optimal control problem. To summarize, we aim to minimize the cost function in Eq (2.2) subject to the yellow fever model in Eq (2.1) as the state system, and the adjoint system in Eq (4.3) with the terminal condition given, and the optimality condition in Eq (4.4). We performed numerical simulations using the forward-backward sweep method [50]. To perform these simulation, we chose the following initial conditions:

$$\begin{aligned}&S(0) = 8500, V(0) = 0, E_1(0) = 800, E_2(0) = 0, I(0) = 500,\\ &T_1(0) = 0, T_2(0) = 0, R(0) = 200, U(0) = 17000, V(0) = 3000.\end{aligned} \tag{4.6}$$

Additionally, to balance each component in the cost function Eq (2.2), we choose $\omega_3 = \omega_4 = \omega_5 = \omega_6 = \omega_7 = 1, \omega_{10} = 0.1, \varphi_1 = 2500, \varphi_2 = 5000$, and $\varphi_3 = 1500$. We use the same parameter values as in the previous section, which gives $\mathscr{R}_0 = 1.504$. Hence, without further improvement in the intervention, yellow fever will be endemic to the population. The autonomous simulation of system (3.1) without any intervention ($u_1(t) = u_2(t) = u_3(t) = 0$) is shown as a red curve in Figures 9–13. We called this simulation as Strategy 0.

For optimal control experiments, we divide our experiments based on the combination of each form of intervention as follows:

- Strategy 1: Vaccination only ($u_1(t) \geq 0, u_2(t) = u_3(t) = 0$).
- Strategy 2: Fumigation only ($u_1(t) = u_2(t) = 0, u_3 \geq 0$).
- Strategy 3: Vaccination and hospitalization only ($u_1(t) \geq 0, u_2(t) \geq 0, u_3(t) = 0$).
- Strategy 4: Vaccination and fumigation only ($u_1(t) \geq 0, u_2(t) = 0, u_3(t) \geq 0$).
- Strategy 5: All interventions implemented ($u_1(t) \geq 0, u_2(t) \geq 0, u_3(t) \geq 0$).

Strategy 1

In the first simulation, the optimal control simulation used vaccination as the only means of intervention. The results are shown in Figure 9.

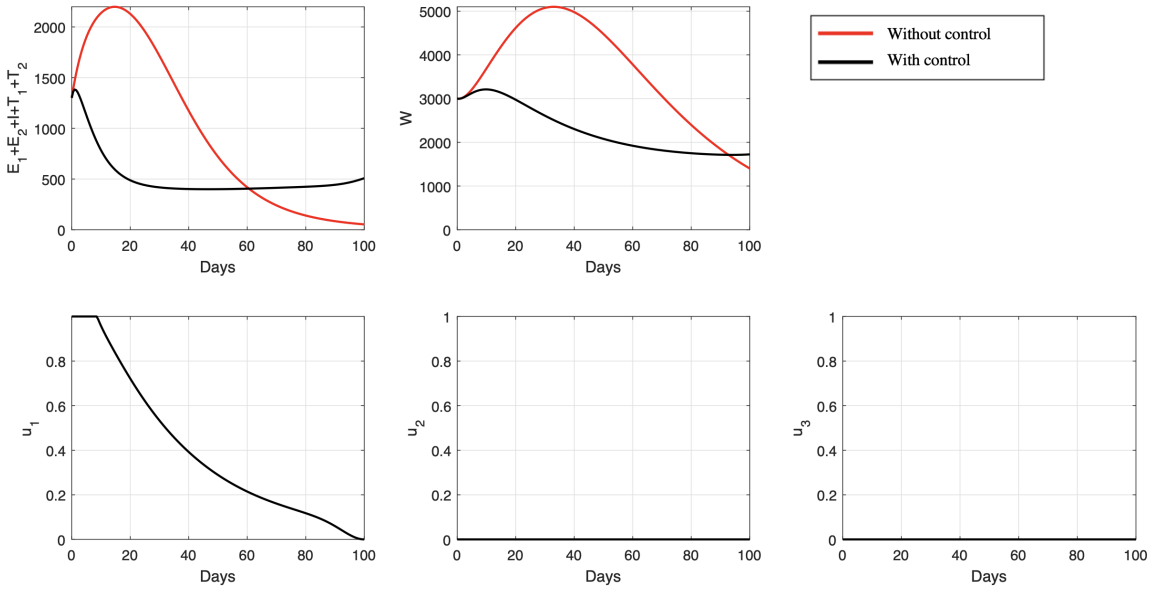

Figure 9. Dynamics of total infected human, infected mosquitoes, and control variables for Strategy 1.

The implementation of vaccination with the greatest effort should be done at the beginning of simulation. It will reduce the number of infected people, reducing both direct contact between vulnerable mosquitoes and infected people and the number of infected mosquitoes. Reducing the level of intervention will cause the number of infected people and mosquitoes to increase near the end of the simulation. Yellow fever vaccines can cause side effects in rare cases; therefore, the total number of infected people rose immediately after vaccination before slowly decreasing toward the end.

Based on maximum vaccination at the start, this strategy has a cost of 632, 377 and prevents 444, 868 infections, leading to a total of 2, 981, 365 recovered individuals.

Strategy 2

The optimal control strategy for this simulation only uses fumigation to control mosquito populations with the aim of breaking the yellow fever infection cycle. The results are shown in Figure 10.

This strategy involves maximum fumigation for nearly three months, before drastically decreasing the rate of fumigation toward the end owing to the rapidly increasing number of infected mosquitoes since the start. This significantly reduced the number of infected people and mosquitoes. Fumigation helps control the number of infected mosquitoes that can come into direct contact with susceptible individuals.

Although this strategy has a cost of 333, 345, which is almost half that of the first strategy, it prevents 784, 547 infections, far more than the first strategy. With this strategy, 1, 819, 666 people will recover by the end of the period.

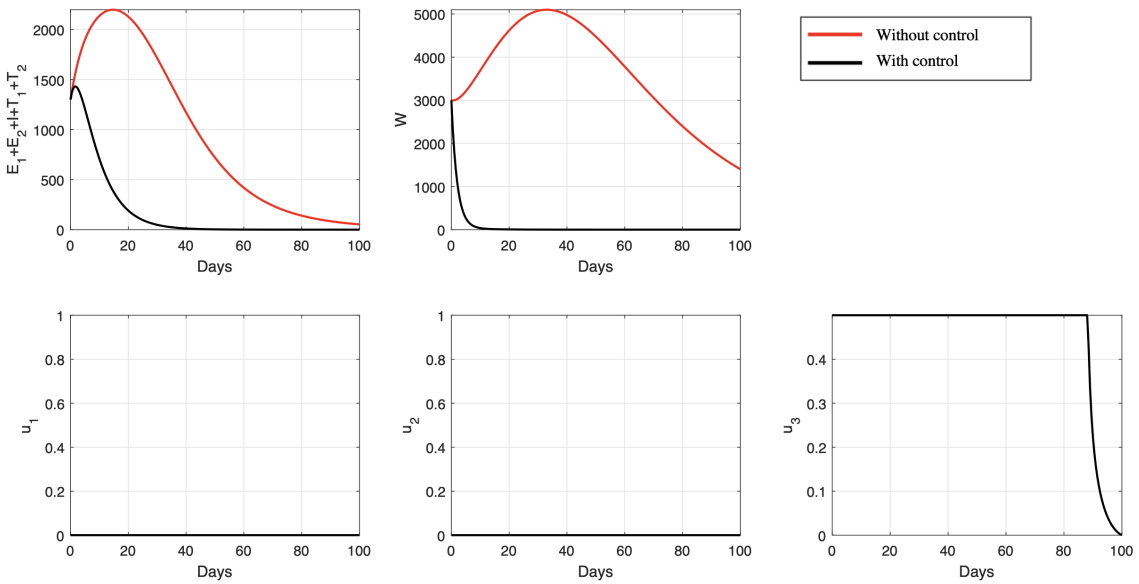

Figure 10. Dynamic of total infected human, infected mosquitoes, and control variables for Strategy 2.

Strategy 3

The third optimal control simulation combines vaccination and treatment. People in T_1 receive treatment to aid in the recovery process. Treatment is given because yellow fever vaccines may cause side effects in rare cases. The results are shown in Figure 11.

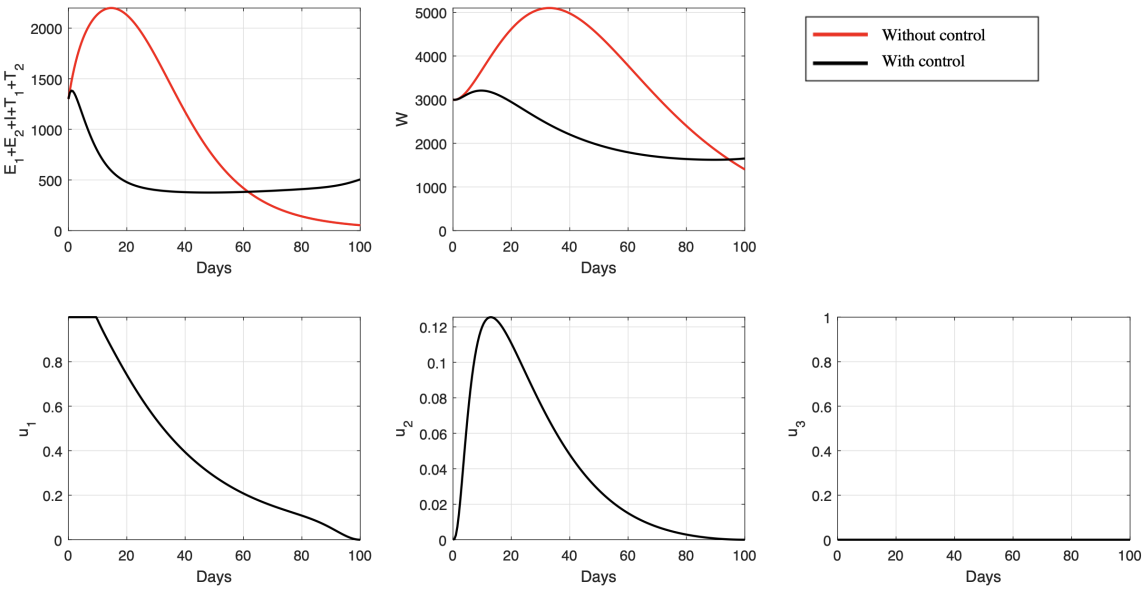

Figure 11. Dynamic of total infected human, infected mosquitoes, and control variables for Strategy 3.

The implementation of vaccination with the greatest effort should be done at the beginning of simulation. It would be accompanied by the side effects of the yellow fever vaccine. Treatment must counteract this effect. Treatment continued until day 14. This reduces the number of infected individuals, which without any intervention will increase until the 30^{th} day. Vaccination is reduced because of the declining number of infected people.

This strategy has a higher cost than the previous two strategies (664, 808) but is only slightly better at preventing infections (458, 867) and yields a similar number of recovered people (2, 949, 196).

Strategy 4

The fourth optimal control simulation uses both vaccination and fumigation to combat yellow fever. The results are shown in Figure 12.

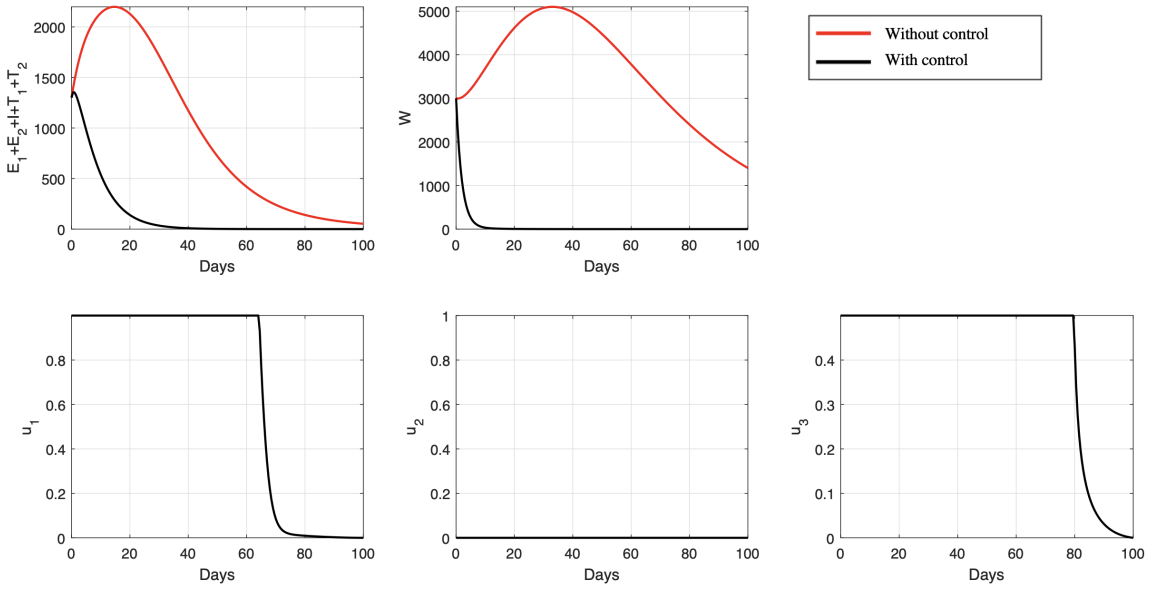

Figure 12. Dynamic of total infected human, infected mosquitoes, and control variables for Strategy 4.

Maximum fumigation and vaccination are given simultaneously for the first 60 days to slow the rise in the number of infected people and mosquitoes.

Maximum intervention throughout the period is impossible because of cost constraints. Therefore, vaccination is reduced after the 65^{th} day, and fumigation is reduced after the 81^{st} day. This strategy causes the number of infected mosquitoes and infected humans to approach zero on the 14^{th} and the 38^{th} days, respectively.

This strategy has the highest cost of all four strategies (1, 933, 426) but yields the same number of prevented infections as the second strategy (815, 668) and fewer recovered individuals than the second strategy (1, 551, 319).

Strategy 5

In the last simulation, the optimal control simulation simultaneously involved all interventions (vaccination, hospitalization, and fumigation) to control the spread of yellow fever. The simulation results

are shown in Figure 13. Note that all interventions must be given to the fullest extent possible from the start of the simulation. Therefore, the number of infected humans and mosquitoes has decreased significantly since the first day. When the infected population in both human and mosquito populations stops increasing, the vaccination, hospitalization, and fumigation interventions will gradually decrease until they reach zero on the final day of the simulation.

With maximum intervention from the beginning of the simulation, the cost function is worth 2694.146, which is much larger than the cost function value in Strategy 4. Nonetheless, when compared to Strategy 4, the number of infected humans successfully avoided was not significantly different, that is, 816 individuals. Similarly, the number of successfully recovered people is not significantly different from Strategy 4, which is 1551 individuals.

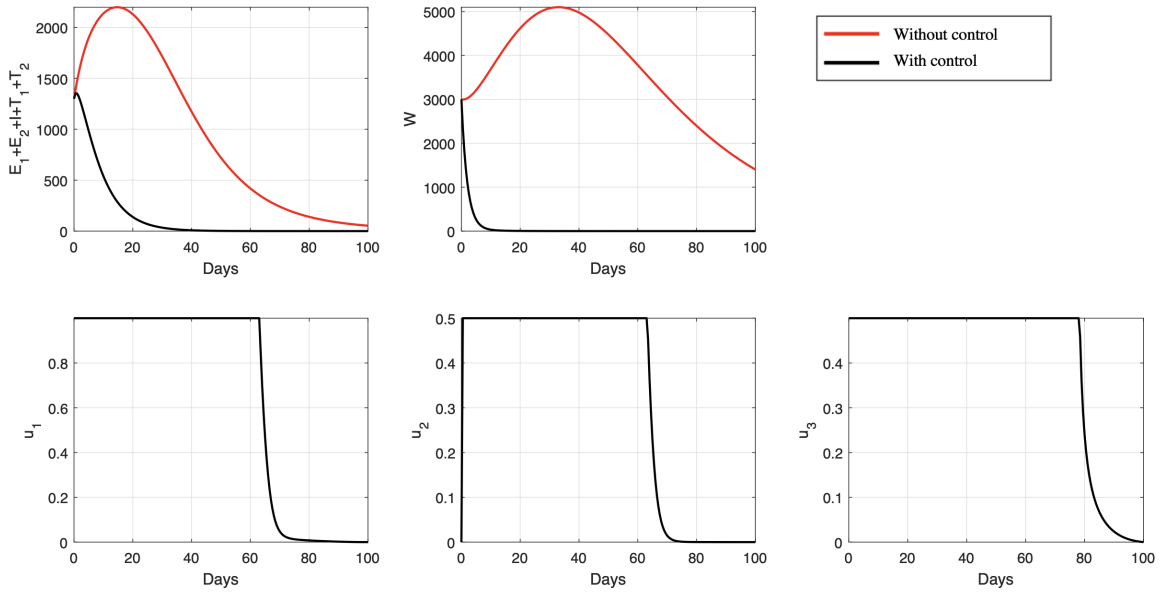

Figure 13. Dynamic of total infected human, infected mosquitoes, and control variables for Strategy 5.

4.3. Cost-effectiveness analysis

It is critical to determine the most cost-effective strategy among the five proposed strategies based on the results of our optimal control simulations. To accomplish this, we use three methods: the average cost-effectiveness ratio (ACER), infected averted ratio (IAR), and incremental cost-effectiveness ratio (ICER) [51–53].

Average cost-effectiveness ratio (ACER)

The ACER method calculates the average cost that should be spent for each number of avoided infected individuals. The ACER formula is as follows:

$$\text{ACER}_{\text{Strategy i}} = \frac{\text{Total cost for intervention with Strategy i}}{\text{Total number of infection averted with Strategy i}}. \tag{4.7}$$

Therefore, a smaller ACER indicates a better strategy. The results of the ACER values for each strategy are shown in Figure 14. Note that the best strategy based on the ACER index implemented fumigation

as a single form of intervention (Strategy 2), followed by Strategies 1, 3, 4, and 5. This means that using fumigation as a single form of intervention is the cheapest way, on average, to avoid many newly infected individuals. An interesting result shows that in our numerical experiment, vaccination is not cost-effective in reducing the expected number of newly infected individuals. This is because in our simulation, the number of infected individuals is already high (13% in the human population and 15% in the mosquito population). Furthermore, the simultaneous implementation of all strategies is not cost-effective because we must increase the already high hospitalization cost further.

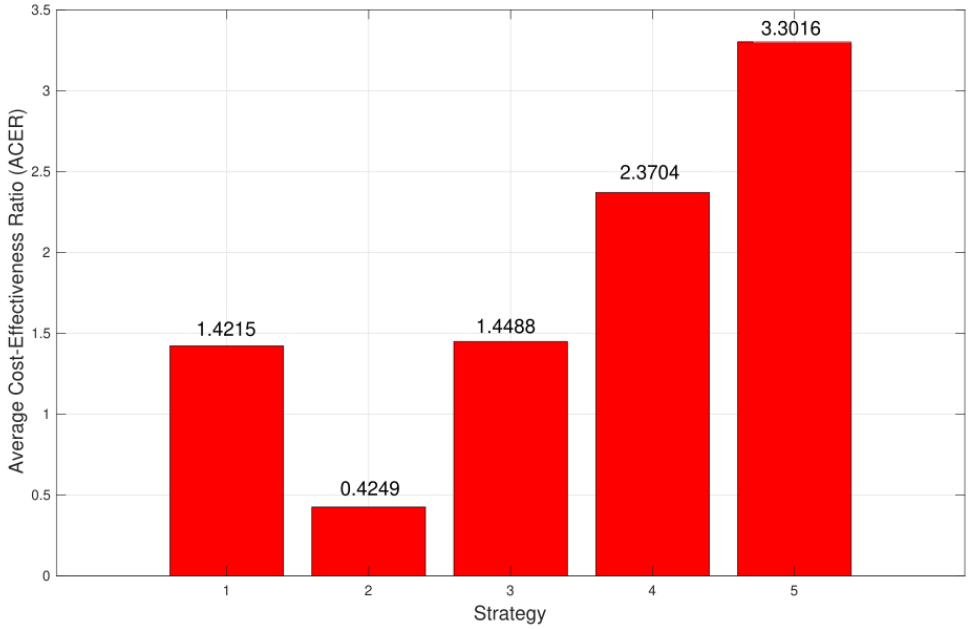

Figure 14. The average cost-effectiveness ratio (ACER) of Strategies 1–5.

Infected averted ratio (IAR)

The IAR method calculates the ratio between the number of infected averted individuals and the number of recovered individuals. The equation for IAR is as follows:

$$\text{IAR}_{\text{Strategy i}} = \frac{\text{Total number of infection averted with Strategy i}}{\text{Total recovered individuals with Strategy i}}. \tag{4.8}$$

Based on the above equation, a larger IAR indicates a better strategy. Figure 15 shows that a combination of all means of interventions (Strategy 5) is the best strategy in terms of IAR, but it is only slightly different from Strategy 4. This is because when vaccination, hospitalization, and fumigation are implemented together, all means of intervention aim to reduce the endemic situation and avoid newly infected individuals. However, as we already discussed in the previous section, Strategy 5 comes at a high cost. The second-best strategy in terms of IAR is Strategy 4, followed by Strategies 2, 3, and 1. Note that implementing vaccination as a single single form of intervention is the least cost-effective strategy in the terms of IAR. This is because this type of intervention is more concerned with prevention rather than endemic reduction.

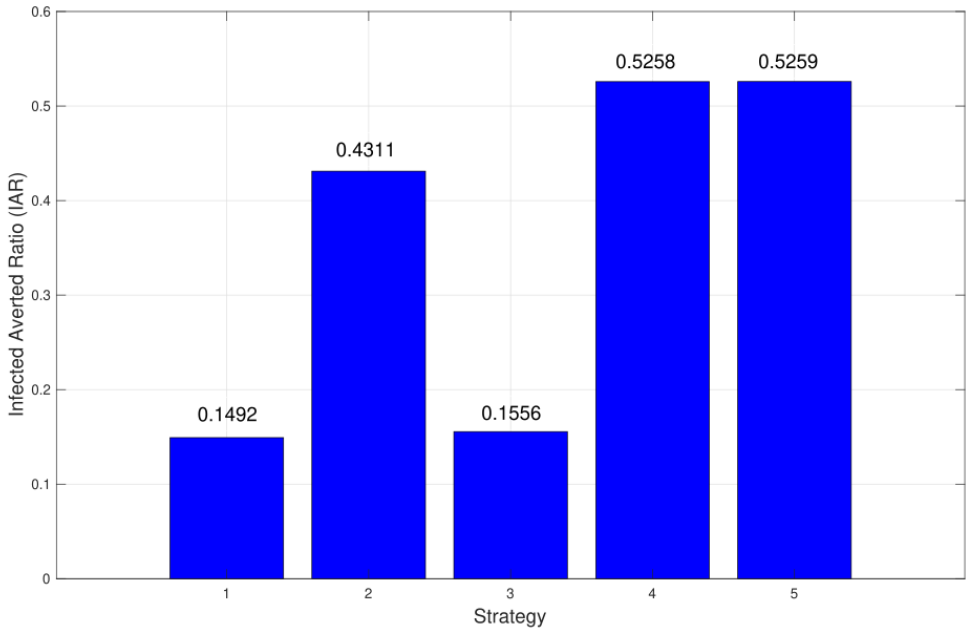

Figure 15. The infected averted ratio (IAR) of Strategies 1–5.

Incremental cost-effectiveness ratio (ICER)

The ICER was the final cost-effectiveness analysis method. The ICER compares the cost differences between two strategies and the number of infected averts. Hence, the equation for ICER is as follows:

$$\text{ICER}_{\text{i–j}} = \frac{\text{Difference of cost between Strategy i and Strategy j}}{\text{Difference of number of infection averted between Strategy i and Strategy j}}. \tag{4.9}$$

Based on the numerical simulation, we rank all strategies in an increasing order based on the total number of infections averted in Table 3. Strategy 1 (intervention of vaccination only) has the lowest number of infections averted, while Strategy 5 (all interventions implemented) has the largest number of infections averted.

Table 3. Strategies 1–5 in increasing order based on the number of infections averted.

Strategy	Total infections averted	Total cost	ICER
Strategy 1	444.868	632.377	1.4215
Strategy 3	458.867	664.808	2.3167
Strategy 2	784.547	333.345	-1.0178
Strategy 4	815.668	1933.426	51.415
Strategy 5	816	2694.146	2285.8173

To compare strategies 1 and 3, the ICER is calculated as follows:

$$\text{ICER} - 1 \quad = \quad \frac{632.377}{444.868} = 1.4215,$$

$$\begin{aligned}
\text{ICER} - 3 &= \frac{664.808 - 632.377}{458.867 - 444.868} = 2.3167,\\
\text{ICER} - 2 &= \frac{333.345 - 664.808}{784.547 - 458.867} = -1.0178,\\
\text{ICER} - 4 &= \frac{1933.426 - 333.345}{815.668 - 784.547} = 51.415,\\
\text{ICER} - 5 &= \frac{2694.146 - 1933.426}{816 - 815.668} = 2285.8173.
\end{aligned}$$

Note that ICER-3 > ICER-1. Hence, we can exclude ICER-3 from the next calculation because it is more costly than ICER-3. Next, we continue our calculation by comparing the ICER between Strategies 1 and 2. The result of calculating ICER using the same method as before is shown in Table 4.

Table 4. Comparison between Strategies 1 and 2.

Strategy	Total infection averted	Total cost	ICER
Strategy 1	444.868	632.377	1.4215
Strategy 2	784.547	333.345	-.88038
Strategy 4	815.668	1933.426	51.415
Strategy 5	816	2694.146	2285.8173

Table 4 shows that ICER-1>ICER-2, which means that Strategy 1 is more costly than Strategy 2. Hence, we exclude Strategy 1 from the next calculation. Up to this step, we have three last candidates for the best strategies, i.e., Strategies 2, 4, and 5. Next, we compare Strategies 2 and 4, the results of which are shown in Table 5.

Table 5. Comparison between Strategies 2 and 4.

Strategy	Total infection averted	Total cost	ICER
Strategy 2	784.547	333.345	0.4249
Strategy 4	815.668	1933.426	51.415
Strategy 5	816	2694.146	2285.8173

Table 5 shows that Strategy 4 is more costly compared to Strategy 2 because ICER-4 > ICER-2. Hence, we exclude Strategy 4 from the next comparison. The results are presented in Table 6.

Table 6. Comparison between Strategies 2 and 5.

Strategy	Total infection averted	Total cost	ICER
Strategy 2	784.547	333.345	0.4249
Strategy 5	816	2694.146	75.0564

Table 6 indicates that ICER-5 > ICER-2, which means that Strategy 5 (all interventions implemented) is more costly compared to Strategy 2 (only fumigation strategy implemented) in reducing the spread of yellow fever. Additionally, Strategy 5 is dominated by Strategy 2, which means that Strategy 5 is less effective compared to Strategy 2. Hence, we can conclude that fumigation, as a single

intervention to reduce the spread of yellow fever, is the most cost-effective strategy compared to other possible strategies.

5. Conclusions

Yellow fever is an acute viral hemorrhagic fever caused by the yellow fever virus of the Flavivirus genus. It is spread by the bite of several types of female mosquitoes (Aedes, Haemagogus) [54]. It is estimated that more than 100,000 cases occur each year, with Africa accounting for more than 60% of all cases. There are three types of yellow fever based on species that interact during the transmission process. The first type is the jungle transmission, where the transmission process involves monkeys and mosquitoes, while the second type, namely, the urban type, involves mosquitoes and humans. The last type, namely the intermediate type, which commonly occurs in Africa, involves mosquitoes, monkeys, and humans in the transmission process [55]. Yellow fever has an incubation period of three to six days, and the symptoms vary, from headache, backache, vomiting, bleeding, and yellow eyes to death [56]. Several means of interventions have been implemented to control the spread of yellow fever, such as vaccination and fumigation. Vaccination for yellow fever is strongly recommended for individuals planning to travel to the yellow fever endemic area. However, there are a few cases where yellow fever vaccination has a side effect on some vulnerable individuals, such as the elderly, pregnant women, etc. [25]. Infected individuals who already have severe symptoms should be hospitalized.

This work introduces a novel optimal control of the yellow fever model based on a ten-dimensional system of ordinary differential equations with a compartmental model approach. Our model includes three possible form of interventions: vaccination, hospitalization, and fumigation. We show that our model is mathematically and biologically well-defined. Our mathematical analysis shows that our model has two possible equilibriums: the yellow fever-free equilibrium point and the yellow fever endemic equilibrium point. We show that the basic reproduction number of our model plays an important role in determining the existence and stability of our equilibrium points. We discovered that the yellow fever-free equilibrium is always locally asymptotically stable when the basic reproduction number is less than one and unstable when it is greater than one. However, the yellow fever endemic equilibrium never exists when the basic reproduction number is less than one and exists (and is stable) when the basic reproduction number is greater than one. Additionally, we found that the endemic size in human and mosquito populations increased rapidly when the basic reproduction number increased. Using the Castillo-Song bifurcation theorem [41], we demonstrated that our model exhibits a forward bifurcation phenomenon at a basic reproduction number of one. Hence, we can conclude that our basic reproduction number becomes a necessary threshold to determine whether yellow fever will be endemic or disappear from the population.

An optimal control problem is then developed and characterized using the Pontryagin maximum principle [49]. We treated our form of interventions (vaccination, hospitalization, and fumigation) as time-dependent variables. We ran our simulations using a forward-backward method [50] for five types of strategies, depending on the possible combination of strategies. The simulation results demonstrated that all means of intervention can eradicate yellow fever. Our sensitivity analysis found that fumigation was the most elastic parameter for determining the basic reproduction number. A cost-effectiveness analysis was conducted to determine the best strategies to prevent the spread of yellow fever. Three types of cost-effectiveness indicators were used: ACER, IAR, and ICER. We found that vaccination

intervention showed the best ACER results, implying that the vaccination strategy as a single intervention provides the lowest average cost required for an averted infection individual. On the other hand, the strategy of combining vaccination, hospitalization, and fumigation showed the best IAR results. Additionally, we found that using fumigation as a single form of intervention shows the best ICER result, which agrees with the ACER result. Therefore, the results of this study can be used by authorities to determine the best strategy to implement in the field to control the spread of yellow fever.

This study considers only three form of interventions: fumigation, vaccination, and hospitalizations. However, some other means of intervention can be chosen as an option, such as using bed nets or mosquito repellents to reduce the mosquito bite. Furthermore, massive vector control such as fumigation, is a high risk because it can trigger mosquitoes' resistance to fumigants. Hence, a mathematical model concerning more means of intervention and the possibility of mosquito resistance could be considered in future work. Last but not least, it is essential to fit our model to the real-life situation by estimating the best fit parameter. Hence, incidence data of yellow fever is essential for conducting parameter estimation into our model.

Acknowledgements

The author would like to thank the anonymous reviewers for his/her valuable comments. This research was funded by the Indonesian RistekBRIN with PDUPT research grant scheme (ID Number: NKB-159/UN2.RST/HKP.05.00/2021), 2021.

Conflict of interest

The authors declare that they have no conflict of interest.

References

1. J. Florczak-Wyspianska, E. Nawotczynska, W. Kozubski, Yellow fever vaccine-associated neurotropic disease (yel-and)–a case report, *Neurol. Neurochir.*, **51** (2017), 101–105. doi: 10.1016/j.pjnns.2016.09.002.
2. *United Nations*, Prevention of Yellow Fever, 2019. Available from: https://www.cdc.gov/yellowfever/prevention/index.html.
3. *United Nations*, Yellow Fever, 2019. Available from: https://www.who.int/news-room/fact-sheets/detail/yellow-fever.
4. J. E. Staples, A. D. Barrett, A. Wilder-Smith, J. Hombach, Review of data and knowledge gaps regarding yellow fever vaccine-induced immunity and duration of protection, *Vaccines*, **5** (2020), 1–7. doi: 10.1038/s41541-020-0205-6.
5. D. Aldila, Analyzing the impact of the media campaign and rapid testing for covid-19 as an optimal control problem in east java, Indonesia, *Chaos, Solitons Fractals*, **141** (2020), 110364. doi: 10.1016/j.chaos.2020.110364.
6. D. Aldila, Optimal control for dengue eradication program under the media awareness effect, *Int. J. Nonlinear Sci. Numer. Simul.*, 2021. doi: 10.1515/ijnsns-2020-0142.

7. D. Aldila, Mathematical model for HIV spreads control program with ART treatment, in *Journal of physics: Conference series*, **974** (2018), 012035.

8. C. A. G. Engelhard, A. P. Hodgkins, E. E. Pearl, P. K. Spears, J. Rychtar, D. Taylor, A mathematical model of Guinea worm disease in Chad with fish as intermediate transport hosts, *J. Theor. Biol.*, **521** (2021), 110683. doi: 10.1016/j.jtbi.2021.110683.

9. Z. Guo, G. Sun, Z. Wang, Z. Jin, L. Li, C. Li, Spatial dynamics of an epidemic model with nonlocal infection, *Appl. Math. Comput.*, **377** (2020), 125158. doi: 10.1016/j.amc.2020.125158.

10. G. Sun, M. Li, J. Zhang, W. Zhang, X. Pei, Z. Jin, Transmission dynamics of brucellosis: Mathematical modelling and applications in China, *Comput. Struct. Biotechnol. J.*, **18** (2020), 3843–3860. doi: 10.1016/j.csbj.2020.11.014.

11. M. Chapwanya, A. Matusse, Y. Dumont, On synergistic co-infection in crop diseases. The case of the Maize Lethal Necrosis Disease, *Appl. Math. Modell.*, **90** (2021), 912–942. doi: 10.1016/j.apm.2020.09.036.

12. Y. Belgaid, M. Helal, A. Lakmeche, E. Venturino, On the stability of periodic solutions of an impulsive system arising in the control of agroecosystems, in *International Symposium on Mathematical and Computational Biology*, (2020), 183–199.

13. M. Kung'aro, L. Luboobi, F. Shahada, Modelling and stability analysis of SVEIRS yellow fever two host model, *Gulf J. Math.*, **3** (2015), 106–129. doi: 10.1016/j.ces.2015.02.038.

14. S. Raimundo, M. Amaku, E. Massad, Equilibrium analysis of a yellow fever dynamical model with vaccination, *Comput. Math. Methods Med.*, **2015** (2015), 482091. doi: 10.1155/2015/482091.

15. U. Danbaba, S. Garba, Stability analysis and optimal control for yellow fever model with vertical transmission, *Int. J. Appl. Comput. Math*, **6** (2020), 1–34. doi: 10.1007/ s40819-020-00860-z.

16. S. Zhao, L. Stone, D. Gao, D. He, Modelling the large-scale yellow fever outbreak in luanda, angola, and the impact of vaccination, *PLoS Negl. Trop. Dis.*, **12** (2018), e0006158. doi: 10.1371/journal.pntd.0006158.

17. F. Agusto, M. Leite, Optimal control and cost-effective analysis of the 2017 meningitis outbreak in Nigeria, *Infect. Dis. Modell.*, **4** (2019), 161–187. doi: 10.1016/j.idm.2019.05.003.

18. M. Bruyand, M. Receveur, T. Pistone, C. Verdiere, R. Thiebaut, D. Malvy, Yellow fever vaccination in non-immunocompetent patients, *Med. Mal. Infect.*, **38** (2008), 524–532. doi: 10.1016/j.medmal.2008.06.031.

19. S. M. Raimundo, M. Amaku, E. Massad, Equilibrium analysis of a yellow fever dynamical model with vaccination, *Comput. Math. Methods Med.*, **2015** (2015), 482091. doi: 10.1155/2015/482091.

20. *Pan American Health Organization/World Health Organization*, Epidemiological update: yellow fever, 2018. Available from: https://reliefweb.int/report/brazil/epidemiological-update-yellow-fever-20-march-2018.

21. F. M. Shearer, C. L. Moyes, D. M. Pigott, O. J. Brady, F. Marinho, A. Deshpande, et al., Global yellow fever vaccination coverage from 1970 to 2016: an adjusted retrospective analysis, *Lancet Infect. Dis.*, **17** (2017), 1209–1217. doi: 10.1016/S1473-3099(17)30419-X.

22. K. W. Blayneh, A. B. Gumel, S. Lenhart, T. Clayton, Backward bifurcation and optimal control in transmission dynamics of West Nile virus, *Bull. Math. Biol.*, **72** (2010), 1006–1028. doi: 10.1007/s11538-009-9480-0.
23. B. Buonomo, R. D. Marca, Optimal bed net use for a dengue disease model with mosquito seasonal pattern, *Math. Methods Appl. Sci.*, **41** (2018), 573–592. doi: 10.1002/mma.4629.
24. M. Andraud, N. Hens, C. Marais, P. Beutels, Dynamic epidemiological models for dengue transmission: a systematic review of structural approaches, *PLoS ONE*, **7** (2012), e49085. doi: 10.1371/journal.pone.0049085.
25. P. Cottin, M. Niedrig, C. Domingo, Safety profile of the yellow fever vaccine stamaril: a 17-year review, *Expert Rev. Vaccines*, **12** (2013), 1351–1368. doi: 10.1586/14760584.2013.836320.
26. D. Aldila, T. Götz, E. Soewono, An optimal control problem arising from a dengue disease transmission model, *Math. Biosci.*, **242** (2013), 9–16. doi: 10.1016/j.mbs.2012.11.014.
27. T. T. Yusuf, D. O. Daniel, Mathematical modelling of yellow fever transmission dynamics with multiple control measures, *Asian Res. J. Math.*, **13** (2019), 1–15. doi: 10.9734/arjom/2019/v13i430112.
28. D. Aldila, M. Angelina, Optimal control problem and backward bifurcation on malaria transmission with vector bias, *Heliyon*, **7** (2021), e06824. doi: 10.1016/j.heliyon. 2021.e06824.
29. B. Handari, F. Vitra, R. Ahya, T. N. S, D. Aldila, Optimal control in a malaria model: intervention of fumigation and bed nets, *Adv. Differ. Equations*, **2019** (2019), 497. doi: 10.1186/s13662-019-2424-6.
30. M. S. Indriyono Tantoro, Pedoman Pencegahan Penyakit Yellow Fever, in *Kementerian Kesehatan Republik Indonesia Direktorat Jenderal Pencegahan dan Pengendalian Penyakit*, 2017.
31. D. Aldila, B. M. Samiadji, G. M. Simorangkir, S. H. A. Khosnaw, M. Shahzad, Impact of early detection and vaccination strategy in covid-19 eradication program in jakarta, indonesia, *BMC Res. Notes*, **14** (2021), 132. doi: 10.1186/s13104–021–05540–9.
32. I. M. Wangaria, S. Davisa, L. Stone, Backward bifurcation in epidemic models: Problems arisingwith aggregated bifurcation parameters, *Appl. Math. Modell.*, **40** (2016), 1669–1675. doi: 10.1016/j.apm.2015.07.022.
33. O. Diekmann, J. A. P. Heesterbeek, M. G. Roberts, The construction of next-generation matrices for compartmental epidemic models, *J. R. Soc. Interface*, **7** (2010), 873–885. doi: 10.1098/rsif.2009.0386.
34. P. van den Driessche, J. Watmough, Reproduction numbers and sub-threshold endemic equilibria for compartmental models of disease transmission, *Math. Biosci.*, **180** (2002), 29–48. doi: 10.1016/S0025-5564(02)00108-6.
35. G. Simorangkir, D. Aldila, A. Rizka, H. Tasman, E. Nugraha, Mathematical model of tuberculosis considering observed treatment and vaccination interventions, *J. Interdiscip. Math.*, **24** (2021), 1717–1737. doi: 10.1080/09720502.2021.1958515.
36. D. Aldila, K. Rasyiqah, G. Ardaneswari, H. Tasman, A mathematical model of zika disease by considering transition from the asymptomatic to symptomatic phase, in *Journal of Physics: Conference Series*, **1821** (2021), 012001. doi: 10.1088/1742-6596/1821/1/012001.

37. D. Aldila, B. Handari, Effect of healthy life campaigns on controlling obesity transmission: A mathematical study, in *Journal of Physics: Conference Series*, **1747** (2021), 012003. doi: 10.1088/1742-6596/1747/1/012003.

38. J. Li, Y. Zhao, S. Li, Fast and slow dynamics of malaria model with relapse, *Math. Biosci.*, **246** (2013), 94–104. doi: 10.1098/rspb.2016.0048.

39. K. Nudee, S. Chinviriyasit, W. Chinviriyasit, The effect of backward bifurcation in controlling measles transmission by vaccination, *Chaos Solitons Fractals*, **123** (2018), 400–412. doi: 10.1016/j.chaos.2019.04.026.

40. O. Sharomi, C. Podder, A. Gumel, E. Elbasha, J. Watmough, Role of incidence function in vaccine-induced backward bifurcation in some HIV models, *Math. Biosci.*, **210** (2007), 436–463. doi: 10.1016/j.mbs.2007.05.012.

41. C. Castillo–Chavez, B. Song, Dynamical models of tuberculosis and their applications, *Math. Biosci. Eng.*, **1** (2014), 361–404. doi: 10.3934/mbe.2004.1.361.

42. N. Chitnis, J. Hyman, J. Cushing, Determining important parameters in the spread of malaria through the sensitivity analysis of a mathematical model, *Bull. Math. Biol.*, **70** (2008), 1272–1296. doi: 10.1007/s11538-008-9299-0.

43. S. H. A. Khosnaw, M. Shahzad, M. Ali, F. Sultan, A quantitative and qualitative analysis of the covid–19 pandemic model, *Chaos, Solitons Fractals*, **138** (2020), 109932. doi: 10.1016/j.chaos.2020.109932.

44. S. H. A. Khosnaw, M. Shahzad, M. Ali, F. Sultan, Mathematical modelling for coronavirus disease (covid-19) in predicting future behaviours and sensitivity analysis, *Math. Model. Nat. Phenom.*, **15** (2020), 33. doi: 10.1016/j.chaos.2020.109932.

45. A. Abidemi, N. Aziz, Optimal control strategies for dengue fever spread in Johor, Malaysia, *Comput. Methods Programs Biomed.*, **196** (2020), 105585. doi: 10.1016/ j.cmpb.2020.105585.

46. D. Aldila, M. Ndii, B. Samiadji, Optimal control on covid-19 eradication program in Indonesia under the effect of community awareness, *Math. Biosci. Eng.*, **17** (2021), 6355–6389. doi: 10.3934/mbe.2020335.

47. N. Sharma, R. Singh, J. Singh, E. Castillo, Modeling assumptions, optimal control strategies and mitigation through vaccination to zika virus, *Chaos, Solitons Fractals*, **150** (2021), 111137. doi: 10.1016/j.chaos.2021.111137.

48. N. Sweilam, S. Al-Mekhlafi, Optimal control for a fractional tuberculosis infection model including the impact of diabetes and resistant strains, *J. Adv. Res.*, **17** (2019), 125–137. doi: 10.3934/mbe.2020335.

49. L. Pontryagin, V. Boltyanskii, R. Gamkrelidze, E. Mishchenko, *The Mathematical Theory of Optimal Processes*, Interscience Publishers John Wiley & Sons, Inc., New York-London.

50. S. Lenhart, J. Workman, *Optimal Control Applied to Biological Models*, Chapman and Hall, London/Boca Raton, 2007.

51. K. Okosun, O. Rachid, N. Marcus, Optimal control strategies and cost-effectiveness analysis of a malaria model, *BioSystems*, **111** (2013), 83–101. doi: 0.1016/j.biosystems.2012.09.008.

52. F. Agusto, I. ELmojtaba, Optimal control and cost-effective analysis of malaria/visceral leishmaniasis co–infection, *PLoS ONE*, **12** (2017), 1–31. doi: 10.1371/journal.pone.0171102.

53. J. Akanni, F. Akinpelu, S. Olaniyi, A. Oladipo, A. Ogunsola, Modelling financial crime population dynamics: optimal control and cost-effectiveness analysis, *Int. J. Dyn. Control*, **2019** (2019), 1–14. doi: 10.1007/s40435-019-00572-3.

54. E. Q. Lima, M. L. Nogueira, Viral hemorrhagic fever-induced acute kidney injury, in *Seminars in Nephrology*, **28** (2008), 409–415. doi: 10.1016/j.semnephrol.2008.04.009.

55. R. Klitting, E. A. Gould, C. Paupy, X. De Lamballerie, What does the future hold for yellow fever virus?, *Genes*, **9** (2018), 291. doi: 10.3390/genes9060291.

56. I. McGuinness, J. D. Beckham, K. L. Tyler, D. M. Pastula, An overview of yellow fever virus disease, *Neurohospitalist*, **7** (2017), 157. doi: 10.1177/1941874417708129.

Appendix

A. Proof of Theorem 1

From yellow fever model in Eq (3.1), with a non-negative initial conditions on each variables, we have the following result:

$$\begin{aligned}
\frac{dS}{dt}\Big|_{S>0,V\geq0,E_1\geq0,E_2\geq0,I\geq0,T_1\geq0,T_2\geq0,R\geq0,U>0,V\geq0} &= \Lambda_h + \omega_h V > 0,\\
\frac{dV}{dt}\Big|_{S>0,V=0,E_1\geq0,E_2\geq0,I\geq0,T_1\geq0,T_2\geq0,R\geq0,U>0,V\geq0} &= u_1 S \geq 0,\\
\frac{dE_1}{dt}\Big|_{S>0,V\geq0,E_1=0,E_2\geq0,I\geq0,T_1\geq0,T_2\geq0,R\geq0,U>0,V\geq0} &= \beta_h S W \geq 0,\\
\frac{dE_2}{dt}\Big|_{S>0,V\geq0,E_1\geq0,E_2=0,I\geq0,T_1\geq0,T_2\geq0,R\geq0,U>0,V\geq0} &= \xi\beta_h V W \geq 0,\\
\frac{dI}{dt}\Big|_{S>0,V\geq0,E_1\geq0,E_2\geq0,I=0,T_1\geq0,T_2\geq0,R\geq0,U>0,V\geq0} &= \gamma_1 E_1 + (1-p)\gamma_2 E_2 \geq 0,\\
\frac{dT_1}{dt}\Big|_{S>0,V\geq0,E_1\geq0,E_2\geq0,I\geq0,T_1=0,T_2\geq0,R\geq0,U>0,V\geq0} &= p\gamma_2 E_2 \geq 0,\\
\frac{dT_2}{dt}\Big|_{S>0,V\geq0,E_1\geq0,E_2\geq0,I\geq0,T_1\geq0,T_2=0,R\geq0,U>0,V\geq0} &= u_2 T_1 \geq 0,\\
\frac{dR}{dt}\Big|_{S>0,V\geq0,E_1\geq0,E_2\geq0,I\geq0,T_1\geq0,T_2\geq0,R=0,U>0,V\geq0} &= \delta_1 I + \delta_2 T_1 + \delta_3 T_2 \geq 0,\\
\frac{dU}{dt}\Big|_{S>0,V\geq0,E_1\geq0,E_2\geq0,I\geq0,T_1\geq0,T_2\geq0,R\geq0,U=0,V\geq0} &= \Lambda_v > 0,\\
\frac{dW}{dt}\Big|_{S>0,V\geq0,E_1\geq0,E_2\geq0,I\geq0,T_1\geq0,T_2\geq0,R\geq0,U>0,V=0} &= \beta_v U(I+T_1) \geq 0.
\end{aligned} \tag{A.1}$$

The above calculation at the boundary of each variable indicates that the rates of each variable are non-negative on the boundary planes of $\mathbb{R}^{10}_+$. Hence, we can conclude that all vector fields in the

boundary are always pointed inward. Therefore, whenever the initial condition is non-negative in $\mathbb{R}^{10}_{+}$, the solution will always remain non-negative for all times $t > 0$. Hence, the proof is complete.

B. Proof of Theorem 2

Because $\frac{dN}{dt} = \Lambda_h - I\alpha_1 - T_1\alpha_2 - T_2\alpha_3 - \mu_h N$, we have

$$\begin{aligned} \frac{dN}{dt} &= \Lambda_h - I\alpha_1 - T_1\alpha_2 - T_2\alpha_3 - N\mu_h, \\ &\leqslant \Lambda_h - \mu_h N. \end{aligned} \tag{B.1}$$

Solve the above equation with respect to $N(t)$, we have the following:

$$N(t) \leqslant N(0)e^{-\mu_h t} + \frac{\Lambda_h}{\mu_h}(1 - e^{-\mu_h t}).$$

Therefore, for $t \to \infty$, $N(t)$ tends to $\dfrac{\Lambda_h}{\mu_h}$. A similar approach can be used to demonstrate that the total mosquito population ($M(t)$) is eventually bounded by $\dfrac{\Lambda_v}{\mu_v}$. Hence, the proof is complete.

C. Derivation of $\mathscr{R}_0$

Taking only the infected compartment in system (3.1), the transmission (**T**) and the transition (Σ) matrix, which are evaluated in $\mathscr{E}_1$, are given by the following:

$$\mathbf{T} = \begin{bmatrix} 0 & 0 & 0 & 0 & 0 & \dfrac{(\mu_h + \omega_h)\Lambda_h\beta_h}{\mu_h(\mu_h + \omega_h + u_1)} \\ 0 & 0 & 0 & 0 & 0 & \dfrac{\xi\beta_h\Lambda_h u_1}{\mu_h(\mu_h + \omega_h + u_1)} \\ 0 & 0 & 0 & 0 & 0 & 0 \\ 0 & 0 & 0 & 0 & 0 & 0 \\ 0 & 0 & 0 & 0 & 0 & 0 \\ 0 & 0 & \dfrac{\beta_v\Lambda_v}{\mu_v + u_3} & \dfrac{\beta_v\Lambda_v}{\mu_v + u_3} & 0 & 0 \end{bmatrix},$$

and

$$\Sigma = \begin{bmatrix} -\gamma_1 - \mu_h & 0 & 0 & 0 & 0 & 0 \\ 0 & a_{22} & 0 & 0 & 0 & 0 \\ \gamma_1 & (1-p)\gamma_2 & -\mu_h - \alpha_1 - \delta_1 & 0 & 0 & 0 \\ 0 & p\gamma_2 & 0 & -\delta_2 - u_2 - \mu_h - \alpha_2 & 0 & 0 \\ 0 & 0 & 0 & u_2 & -\delta_3 - \mu_h - \alpha_3 & 0 \\ 0 & 0 & 0 & 0 & 0 & -\mu_v - u_3 \end{bmatrix},$$

where $a_{22} = -(1-p)\gamma_2 - p\gamma_2 - \mu_h$. Using the formula in [33], the next generation matrix of system (3.1) is given by $\mathbf{K} = -E^t\mathbf{T}\Sigma^{-1}E$, where

$$\mathbf{E} = \begin{bmatrix} 1 & 0 & 0 \\ 0 & 1 & 0 \\ 0 & 0 & 0 \\ 0 & 0 & 0 \\ 0 & 0 & 0 \\ 0 & 0 & 1 \end{bmatrix}, \mathbf{E}^t = \begin{bmatrix} 1 & 0 & 0 & 0 & 0 & 0 \\ 0 & 1 & 0 & 0 & 0 & 0 \\ 0 & 0 & 0 & 0 & 0 & 1 \end{bmatrix}.$$

Hence, the basic reproduction number of system (3.1) as the spectral radius of $\mathbf{K}$ is given by the following:

$$\mathscr{R}_0 = \rho(\mathbf{K}) = \frac{\sqrt{\mu_h(\alpha_2+\delta_2+\mu_h+u_2)(\gamma_1+\mu_h)M_1}}{\mu_h(\mu_h+\omega_h+u_1)(\gamma_2+\mu_h)(\mu_v+u_3)(\gamma_1+\mu_h)(\alpha_2+\delta_2+\mu_h+u_2)(\alpha_1+\delta_1+\mu_h)}, \quad \text{(C.1)}$$

with

$$\begin{aligned} M_1 =& (\gamma_1\mu_h^3 + ((\xi u_1+\gamma_1)\gamma_2 + \gamma_1(\delta_2+\omega_h+u_2+\alpha_2))\mu_h^2 + (((\xi u_1+\alpha_2+\delta_2+\omega_h+u_2)\gamma_1 + u_1(p\alpha_1+p\delta_1 \\ &+ (\alpha_2+\delta_2+u_2)(1-p))\xi)\gamma_2 + \gamma_1\omega_h(\alpha_2+\delta_2+u_2))\mu_h + \gamma_1\gamma_2(u_1(p\alpha_1+p\delta_1+(\alpha_2+\delta_2+u_2)(1-p)) \\ &\xi + \omega_h(\alpha_2+\delta_2+u_2)))\Lambda_v\beta_v(\mu_h+\omega_h+u_1)(\gamma_2+\mu_h)\beta_h(\alpha_1+\delta_1+\mu_h)\Lambda_h. \end{aligned}$$

D. The proof of Theorem 3

Let us simplify the notion of $E_1, E_2, I, T_1, T_2, W, R, S, V, U$ as x_i for $i = 1, 2, \ldots 10$, respectively. We redefine system (3.1) as follows:

$$\begin{aligned} f_1 := \frac{dE_1}{dt} &= \beta_h S W - \gamma_1 E_1 - \mu_h E_1, \\ f_2 := \frac{dE_2}{dt} &= \xi\beta_h V W - (1-p)\gamma_2 E_2 - p\gamma_2 E_2 - \mu_h E_2, \\ f_3 := \frac{dI}{dt} &= \gamma_1 E_1 + (1-p)\gamma_2 E_2 - (\mu_h+\alpha_1)I - \delta_1 I, \\ f_4 := \frac{dT_1}{dt} &= p\gamma_2 E_2 - \delta_2 T_1 - u_2 T_1 - (\mu_h+\alpha_2)T_1, \\ f_5 := \frac{dT_2}{dt} &= u_2 T_1 - \delta_3 T_2 - (\mu_h+\alpha_3)T_2, \\ f_6 := \frac{dW}{dt} &= \beta_v U(I+T_1) - (\mu_v+u_3)W, \\ f_7 := \frac{dR}{dt} &= \delta_1 I + \delta_2 T_1 + \delta_3 T_2 - \mu_h R, \\ f_8 := \frac{dS}{dt} &= \Lambda_h + \omega_h V - \beta_h S W - u_1 S - \mu_h S, \\ f_9 := \frac{dV}{dt} &= u_1 S - \xi\beta_h V W - \mu_h V - \omega_h V, \\ f_{10} := \frac{dU}{dt} &= \Lambda_v - \beta_v U(I+T_1) - (\mu_v+u_3)U. \end{aligned} \quad \text{(D.1)}$$

Now, we define our yellow-fever free equilibrium as

$$\begin{aligned}\mathbf{X_s} &= (x_1, x_2, x_3, x_4, x_5, x_6, x_7, x_8, x_9, x_{10}),\\ &= \left(0,0,0,0,0,0,0,\frac{\lambda_h(\mu_h+\omega_h)}{\mu_h(\mu_h+\omega_h+u_1)},\frac{\Lambda_h u_1}{\mu_h(\mu_h+\omega_h+u_1)},\frac{\Lambda_v}{\mu_v+u_3}\right).\end{aligned} \tag{D.2}$$

To apply Theorem 2 in [34], we have to show that the system (D.1) satisfies five axioms in [34]. Therefore, we need to separate the infection ($\mathcal{F}$) and the non-infection ($\mathcal{V}$) term in the symstem (D.1) as follows:

$$\mathcal{F} = \begin{bmatrix} WS\beta_h \\ \xi\beta_h VW \\ 0 \\ 0 \\ 0 \\ \beta_v U(I+T_1) \\ 0 \\ 0 \\ 0 \\ 0 \end{bmatrix}, \quad \mathcal{V} = \begin{bmatrix} (\gamma_1+\mu_h)E_1 \\ (1-p)\gamma_2 E_2 + (p\gamma_2+\mu_h)E_2 \\ -\gamma_1 E_1 - (1-p)\gamma_2 E_2 + (\mu_h+\alpha_1)I + \delta_1 I \\ -p\gamma_2 E_2 + (\delta_2+u_2)T_1 + (\mu_h+\alpha_2)T_1 \\ -u_2 T_1 + \delta_3 T_2 + (\mu_h+\alpha_3)T_2 \\ (\mu_v+u_3)W \\ \mu_h R - \delta_1 I - \delta_2 T_1 - \delta_3 T_2 \\ -\Lambda_h - \omega_h V + \beta_h WS + (u_1+\mu_h)S \\ -u_1 S + \xi\beta_h VW + (\mu_h+\omega_h)V \\ -\Lambda_v + \beta_v U(I+T_1) + (\mu_v+u_3)U \end{bmatrix}. \tag{D.3}$$

Note that $\mathcal{V}_i$ can be decomposed as $\mathcal{V}_i = \mathcal{V}_i^- - \mathcal{V}_i^+$, where $\mathcal{V}_i^-$ and $\mathcal{V}_i^+$ represent the out and in flow in compartment-i, respectively. Now, we are ready to proof the five axioms in [34].

1. *If all compartment (x_i, $i = 1, 2, \ldots 10$) are non-negative, then $\mathcal{F}_i, \mathcal{V}_i^-$, and $\mathcal{V}_i^+$ are always non-negative*. By substituting $x_i \geq 0$ into $\mathcal{F}_i, \mathcal{V}_i^-$, and $\mathcal{V}_i^+$, we can verify that $\mathcal{F}_i, \mathcal{V}_i^-$, and $\mathcal{V}_i^+$ are always non-negative.
2. *If all compartments are empty, then there is no out-flow rate from each compartment.* It is easy to verify that, $\mathcal{V}_i^- = 0$ for $i = 1, 2, \ldots 10$ when we set $x_i = 0$ for $i = 1, 2, \ldots 10$.
3. *For all non infected compartment (x_i, $i = 7, 8, 9, 10$), we have that $\mathcal{F}_i = 0$.* This axiom satisfies directly by the expression of $\mathcal{F}$ at (D.3).(?)
4. *If $x_i \in \mathbf{X_s}$, then $\mathcal{F}_i = 0 = \mathcal{V}_i^+ = 0$ for $i = 1, 2, \ldots 6$.* By substituting $\mathbf{X_s}$ into $\mathcal{F}_i$, $i = 1, 2, \ldots 6$, we have that $\mathcal{F}_i = 0$ and $\mathcal{V}_i^+ = 0$, $i = 1, 2, \ldots 6$.
5. *If $\mathcal{F}(x) = 0$, then all the eigenvalues of $Df(\mathbf{X_s})$ have a negative real part, where $Df(\mathbf{X_s})$ is the Jacobian matrix of* (D.1) *evaluated at* $\mathbf{X_s}$. By substituting $\mathbf{X_s}$ into system (D.1), we obtain :

$$\begin{aligned} f_1 = \frac{dE_1}{dt} &= -\gamma_1 E_1 - \mu_h E_1,\\ f_2 = \frac{dE_2}{dt} &= -(1-p)\gamma_2 E_2 - p\gamma_2 E_2 - \mu_h E_2,\\ f_3 = \frac{dI}{dt} &= \gamma_1 E_1 + (1-p)\gamma_2 E_2 - (\mu_h+\alpha_1)I - \delta_1 I,\\ f_4 = \frac{dT_1}{dt} &= \gamma_2 E_2 - \delta_2 T_1 - u_2 T_1 - (\mu_h+\alpha_2)T_1,\\ f_5 = \frac{dT_2}{dt} &= u_2 T_1 - \delta_3 T_2 - (\mu_h+\alpha_3)T_2, \end{aligned} \tag{D.4}$$

$$
\begin{aligned}
f_6 = \frac{dW}{dt} &= -(\mu_v + u_3)W, \\
f_7 = \frac{dR}{dt} &= \delta_1 I + \delta_2 T_1 + \delta_3 T_2 - \mu_h R, \\
f_8 = \frac{dS}{dt} &= \Lambda_h + \omega_h V - \beta_h S W - u_1 S - \mu_h S, \\
f_9 = \frac{dV}{dt} &= u_1 S - \xi\beta_h V W - \mu_h V - \omega_h V, \\
f_{10} = \frac{dU}{dt} &= \Lambda_v - \beta_v U(I + T_1) - (\mu_v + u_3)U.
\end{aligned}
$$

Then, we can evaluate $Df(\mathbf{X_s})$ of system (D.4). By standard calculation, we obtain the eigenvalues of $Df(\mathbf{X_s})$ as follows:

$$
\begin{aligned}
&\lambda_1 = -\mu_h, \quad \lambda_2 = -\mu_h, \quad \lambda_3 = -(\mu_v + u_3), \quad \lambda_4 = -(\mu_v + u_3), \quad \lambda_5 = -(\gamma_2 + \mu_h), \\
&\lambda_6 = -(\gamma_1 + \mu_h), \quad \lambda_7 = -(\alpha_3 + \delta_3 + \mu_h), \quad \lambda_8 = -(u_2 + \alpha_2 + \delta_2 + \mu_h), \\
&\lambda_9 = -(\omega_h + u_1 + \mu_h), \quad \lambda_{10} = -(\alpha_1 + \delta_1 + \mu_h).
\end{aligned}
$$

Since all parameter values are non-negative, we can see that all eigenvalues of $Df(\mathbf{X_s})$ are negative.

Hence, the proof is completed.

E. The proof of Theorem 4

From the expression of $F(W)$ in Eq (3.5), we can see that a_2 is always positive, whereas $a_0 < 0 \iff \mathscr{R}_0^2 > 1$. Using the formula for the multiplication of roots in a second-degree polynomial, we have $W_1^\ddagger \times W_2^\ddagger = \frac{a_0}{a_2}$, where $W_1^\ddagger$ and $W_2^\ddagger$ is the root of $F(W)$. Hence, if $\mathscr{R}_0^2 > 1$, we have $W_1^\ddagger \times W_2^\ddagger < 0$, which indicates that there exists one positive root, and the other one is negative. Therefore, we have a unique yellow fever endemic equilibrium point when $\mathscr{R}_0^2 > 1 \iff \mathscr{R}_0 > 1$.

Now, we analyze the possibility of the existence of $\mathscr{E}_2$ when $\mathscr{R}_0^2 < 1$. To accomplish this, we use the properties of the second-degree polynomial to have two positive roots, that is, $W_1^\ddagger \times W_2^\ddagger = \frac{a_0}{a_2} > 0$, $W_1^\ddagger + W_2^\ddagger = -\frac{a_1}{a_2} > 0$, and $a_1^2 - 4a_2a_0 \geq 0$. However, because the expressions of a_2, a_1, and a_0 is not simple, the expression of $a_1^2 - 4a_2a_0$ is not easy to analyze. Hence, we use another approach to analyze the existence of $\mathscr{E}_2$ when $\mathscr{R}_0 < 1$. To accomplish this, we use a gradient analysis of W in $\mathscr{R}_0 = 1$ and $W = 0$. If we can find a condition such that $\frac{\partial W}{\partial \mathscr{R}_0} < 0$, we can have at least one positive root of $F(W)$ when $\mathscr{R}_0 < 1$. Because the expression of $\mathscr{R}_0$ contains a square root, and the condition of $\mathscr{R}_0 = 1$ is represented by $\mathscr{R}_0^2 = 1$, we will analyze the gradient of W with respect to $\mathscr{R}_0^2$ at $\mathscr{R}_0^2 = 1$ instead of $\mathscr{R}_0 = 1$.

Solving the expression of $\mathscr{R}_0^2 = 1$ in Eq (3.3) with respect to β_h, and substituting it with $F(W)$, we have a_2, a_1, and a_0, which is an expression of $\mathscr{R}_0^2$. Taking the implicit derivative of W with respect to $\mathscr{R}_0^2$ from $F(W)$, we have the following:

$$
\frac{\partial a_2}{\partial \mathscr{R}_0^2}(W^\ddagger)^2 + a_2(2W^\ddagger)\frac{\partial W^\ddagger}{\partial \mathscr{R}_0^2} + \frac{\partial a_1}{\partial \mathscr{R}_0^2}W^\ddagger + a_1\frac{\partial W^\ddagger}{\partial \mathscr{R}_0^2} + \frac{\partial a_0}{\partial \mathscr{R}_0^2} = 0. \tag{E.1}
$$

substitute $W = 0$, and solve it with respect to $\dfrac{\partial W^{\ddagger}}{\partial \mathscr{R}_0^2}$, we have the following:

$$\frac{\partial W^{\ddagger}}{\partial \mathscr{R}_0^2} = -\frac{\dfrac{\partial a_0}{\partial \mathscr{R}_0^2}}{a_1} > 0,$$

where $\dfrac{\partial a_0}{\partial \mathscr{R}_0^2} = -2\,\mu_h(\mu_v + u_3)^2(\gamma_2 + \mu_h)(\gamma_1 + \mu_h)(\alpha_2 + \delta_2 + \mu_h + u_2)(\mu_h + \omega_h + u_1)(\alpha_1 + \delta_1 + \mu_h) < 0$ and $a_1 > 0$. Hence, the gradient of W at $\mathscr{R}_0^2 = 1$ is always positive without any condition. Therefore, we can conclude that there is no yellow fever endemic equilibrium when $\mathscr{R}_0 < 1$. Hence, the proof is complete.

AIMS Press